(This is a sample cover image for this issue. The actual cover is not yet available at this time.)

Deep-Sea Research I 74 (2013) 48–63

Contents lists available at SciVerse ScienceDirect

Deep-Sea Research I

journal homepage: www.elsevier.com/locate/dsri

Changes in deep-water CO_2 concentrations over the last several decades determined from discrete pCO_2 measurements

Rik Wanninkhof [a,*], Geun-Ha Park [a,b,1], Taro Takahashi [c], Richard A. Feely [d], John L. Bullister [d], Scott C. Doney [e]

[a] Atlantic Oceanographic and Meteorological Laboratory of NOAA, 4301 Rickenbacker Cswy., Miami, FL 33149, USA
[b] Cooperative Institute for Marine and Atmospheric Studies, University of Miami, 4600 Rickenbacker Cswy., Miami, FL 33149, USA
[c] Lamont-Doherty Earth Observatory of Columbia University, Route 9W, Palisades, NY 10964, USA
[d] Pacific Marine Environmental Laboratory of NOAA, 7600 Sand Point Way NE, Seattle, WA 98115, USA
[e] Marine Chemistry and Geochemistry Department, Woods Hole Oceanographic Institution, Woods Hole, MA 02543, USA

ARTICLE INFO

Article history:
Received 31 March 2012
Received in revised form
21 December 2012
Accepted 30 December 2012

Keywords:
Ocean
Carbon dioxide
CO_2 sink
Anthropogenic carbon
Deep-water

ABSTRACT

Detection and attribution of hydrographic and biogeochemical changes in the deep ocean are challenging due to the small magnitude of their signals and to limitations in the accuracy of available data. However, there are indications that anthropogenic and climate change signals are starting to manifest at depth. The deep ocean below 2000 m comprises about 50% of the total ocean volume, and changes in the deep ocean should be followed over time to accurately assess the partitioning of anthropogenic carbon dioxide (CO_2) between the ocean, terrestrial biosphere, and atmosphere. Here we determine the changes in the interior deep-water inorganic carbon content by a novel means that uses the partial pressure of CO_2 measured at 20 °C, $pCO_2(20)$, along three meridional transects in the Atlantic and Pacific oceans. These changes are measured on decadal time scales using observations from the World Ocean Circulation Experiment (WOCE)/World Hydrographic Program (WHP) of the 1980s and 1990s and the CLIVAR/CO_2 Repeat Hydrography Program of the past decade. The $pCO_2(20)$ values show a consistent increase in deep water over the time period. Changes in total dissolved inorganic carbon (DIC) content in the deep interior are not significant or consistent, as most of the signal is below the level of analytical uncertainty. Using an approximate relationship between $pCO_2(20)$ and DIC change, we infer DIC changes that are at the margin of detectability. However, when integrated on the basin scale, the increases range from 8–40% of the total specific water column changes over the past several decades. Patterns in chlorofluorocarbons (CFCs), along with output from an ocean model, suggest that the changes in $pCO_2(20)$ and DIC are of anthropogenic origin.

Published by Elsevier Ltd.

1. Introduction

The total anthropogenic carbon dioxide (CO_2) content in the world's ocean has been established to within an uncertainty of 10–15% (e.g. Sabine and Tanhua, 2009; Khatiwala et al., 2009, 2012). The methods of quantifying these changes require a means to separate natural and climate-induced changes in ocean inorganic carbon from that caused by the penetration of anthropogenic CO_2 from the atmosphere (Gruber et al., 1996). The inaccuracy of the measurements commonly used to determine CO_2 concentrations in the ocean makes it difficult to quantify small changes in deep water (depth $\approx >2000$ m) removed from the outcrop regions, referred to as the ocean interior.

There is increasing evidence of physical changes in the deep ocean attributed to increasing atmospheric CO_2 levels and associated climate change. In particular, there are small, but clearly discernible changes in deep-water temperatures (e.g. Johnson and Doney, 2006; Purkey and Johnson, 2010). However, the methods to determine decadal changes in anthropogenic CO_2 in the ocean do not lend themselves to assessment of small changes in the interior deep water because either the uncertainty in the measurements is too great or the methods implicitly or explicitly assume no changes in the ocean interior (Brewer et al., 1983; Peng et al., 1998; Vázquez-Rodríguez et al., 2009). That is, some of the methods assume *a priori* that the anthropogenic imprint in the deep ocean is insignificant and that the biogeochemical processes in deep water have not changed over time. Compounding the challenge of determining small changes in deep water is

* Corresponding author. Tel.: +1 305 361 4379; fax: +1 305 361 4392.
E-mail address: rik.wanninkhof@noaa.gov (R. Wanninkhof).
[1] Current address: East Sea Research Institute, Korea Institute of Ocean Science & Technology, Ulgin, South Korea.

0967-0637/$ - see front matter Published by Elsevier Ltd.
http://dx.doi.org/10.1016/j.dsr.2012.12.005

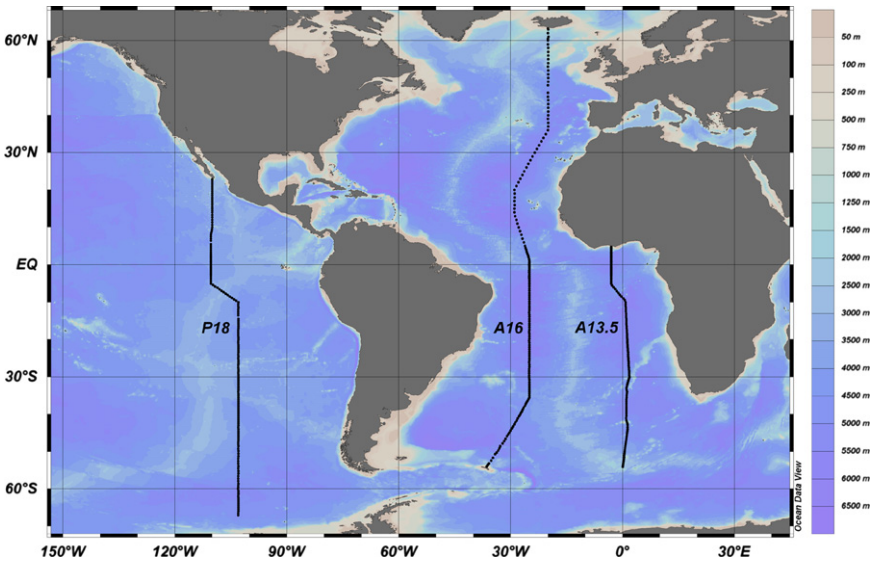

Fig. 1. Station locations for the A16, A13.5, and P18 transects, which are meridional cruises in the central Atlantic, eastern South Atlantic, and eastern South Pacific, respectively. The bathymetry highlighting the ocean ridges is provided with the color scale on the right.

that measurements from different hydrographic surveys are often normalized to deep-water values to adjust for cruise-to-cruise biases (Key et al., 2004).

Determining if anthropogenic carbon has entered the ocean interior is of importance because of the large volume of the deep sea (Garzoli et al., 2010), such that even small increases in concentration can have an appreciable effect on the total water column inventory. Deep-water measurements in ventilation and outcrop regions at higher latitudes have shown deep-water changes attributed to anthropogenic CO_2 (Hoppema et al., 1998; Körtzinger et al., 1999; Tanhua et al., 2006; Pérez et al., 2008; van Heuven et al., 2011; Ríos et al., 2011). In the ocean interior, the signal is below the detection limit using common approaches. Other means to better understand the penetration pathways and storage patterns of anthropogenic CO_2 in the deep ocean are desirable, particularly because on longer time scales the deep water will be the major depository of anthropogenic CO_2.

Here we assess the changes in inorganic carbon using a parameter, "discrete pCO_2," that has not been used before in this context. It is the measurement of the partial pressure of CO_2 from individual subsurface seawater samples made at a fixed temperature of 20 °C, $pCO_2(20)$, and it represents the concentration of undissociated CO_2 molecules dissolved in seawater. The signal to noise of this measurement is currently five-to-eight fold greater than for the state variables, total dissolved inorganic carbon (DIC) and total alkalinity (TAlk), which are the key parameters used to determine anthropogenic CO_2 increases in the ocean. An observed change in $pCO_2(20)$ in deep water is not by itself a definitive indicator of anthropogenic CO_2 but, when used with other parameters such as chlorofluorocarbons (CFCs) and oxygen (O_2), changes can be attributed to either natural or anthropogenic causes. More details about the characteristics and basin-scale patterns of $pCO_2(20)$ in the ocean can be found in Appendix A.

In this investigation, changes in discrete pCO_2 are determined in the deep ocean for two meridional hydrographic sections in the Atlantic (commonly referred to as lines A16 and A13.5) and one in the eastern South Pacific (line P18) using repeat measurements along these lines taken more than a decade apart (Fig. 1, Table 1). These transects have different characteristics with respect to water mass age and ventilation; they are the only sections in the deep ocean where discrete $pCO_2(20)$ measurements were taken using a similar approach by the same investigators. Associated deep-water changes in CFCs are used to speculate on the cause of the changes in deep water. Because of data quality limitations and assumptions discussed in the text and Appendix B, the results are close to the detection limit and are presented on a large scale. The outputs from a numerical ocean circulation model with a biogeochemistry module, the Community Earth System Model (CESM1-BGC) of the National Center for Atmospheric Research (NCAR), sampled along the three hydrographic sections are used for interpretation.

Table 1
Cruises used in the analysis[a].

Cruise section	Cruise name Expocode[b]	Dates	Waypoints (in direction of travel)
Atlantic: 10-years northern section; 16-years southern section			
A16	SAVE5	2/1/1989	32°S
	318MSAVE5	2/17/1989	54°S
	SAVE6 HYDROS4	3/21/1989	32°S
	318MHYDROS4	4/8/1989	0°S
	OACES N.ATL-93	7/8/1993	5°S
	32MB19930708[c]	8/30/1993	64°N
	CLIVAR/CO_2 A16N	6/19/2003	64°N
	33RO20030604	8/9/2003	6°S
	CLIVAR/CO_2 A16S	1/17/2005	50°S
	33RO20050111	2/21/2005	2°S
Eastern S Atlantic: 26-years			
A13.5:	AJAX[d]	10/07/1983	4.8°N
	316N19831007	10/31/1983	45°S
		1/29/1984	69.4°S
	CLIVAR/CO_2 A13.5	3/14/2010	54°S
	33RO20100314[c]	4/17/2010	4.7°N
Pacific: 14-years			
P18	CGC-94:	2/25/1994	61°S
	31DS19940126	4/25/1994	61°S
	CLIVAR/CO_2 P18:	12/17/2007	22.8°N
	33RO20071215	2/16/2008	67°S

[a] Data from: 〈http://cdiac.ornl.gov/oceans/RepeatSections/clivar_table_inv.html〉.
[b] As provided in CARINA, GLODAP, and PACIFICA syntheses.
[c] Created for this table following standard EXPO code annotation.
[d] Chipman et al. (1986).

2. Description of cruises and instrumental analyses

The earlier occupations of the A16, A13.5, and P18 lines occurred as part of the World Hydrographic Program (WHP) of the World Ocean Circulation Experiment (WOCE), while the more recent occupations have been part of the CLIVAR/CO_2 Repeat Hydrography Program. The cruise lines for this study were selected based on the availability of $pCO_2(20)$ and CFC data for both time periods. In particular, there are limited observations of $pCO_2(20)$ and methodological differences in analyses for the surveys (Chen et al., 1995; Neil et al., 1997). The cruises chosen were the only ones where pCO_2 measurements were made by similar approaches by the groups led by the authors. The cruise tracks for the three lines are shown in Fig. 1, and the particulars of each cruise are presented in Table 1.

The initial occupation of the A16 line was a composite of sections in the South Atlantic Ocean occupied in 1989 as part of the South Atlantic Ventilation Experiment, SAVE cruises, and of the A16N section in the North Atlantic occupied in 1993. The repeat of the A16 line consisted of reoccupations of the A16S section in 2005 and the A16N section in 2003. The first occupation of the A13.5 line (called AJAX) occurred in 1983 as a pre-WOCE/WHP cruise. The A13.5 line was reoccupied in 2010 as a CLIVAR/CO_2 cruise. The 1983 AJAX section is one of the first repeated transects with quality $pCO_2(20)$ and CFC measurements (Chipman et al., 1986). It also has the longest time interval between occupations. The P18 line in the eastern Pacific Ocean was occupied in 1994 during WOCE/WHP and in 2007/2008 as part of the CLIVAR/CO_2 Repeat Hydrography Program.

Seawater samples were obtained with 10- to 12-liter Niskin type bottles connected to a frame that housed a CTD (conductivity, temperature, depth) monitor. Samples were obtained at 24 to 36 depths throughout the water column with a horizontal spacing between stations that ranged from 0.25 to 1 degree. Select bottles were subsampled on deck for analyses of the different chemical parameters. The DIC analyses were performed with a coulometer connected to a Single Operator Multi-parameter Metabolic Analyzer, SOMMA (Johnson et al., 1987), following the procedures outlined in the *Handbook of Analysis of Carbon Parameters in Seawater* (DOE, 1994). The accuracy of the DIC analyses was estimated at 2 μmol kg^{-1}, except for the AJAX cruise of 1983 that preceded the availability of certified reference materials to confirm accuracy.

Dissolved chlorofluorocarbons (CFC11 and CFC12) in seawater samples were extracted using purge-and-trap techniques and analyzed in a gas chromatograph equipped with an electron capture detector (Bullister and Weiss, 1988). On the earlier cruises, the CFC analytical blank limited the minimal detectable level attributed to an actual CFC concentration in the sample to ~0.01 pmol kg^{-1} (1 pmol = 10^{-12} moles), but the blank decreased to 0.005 pmol kg^{-1} for the CLIVAR/CO_2 cruises. The high blank for the earlier cruises was attributed to background contamination due to copious amounts of CFCs on ships before CFC11 and CFC12 were phased out as refrigerants. The analyses of $pCO_2(20)$ were performed by circulating the headspace of the 500 ml volumetric flask containing the water sample at 20 °C through a CO_2 analyzer (either an infrared analyzer or gas chromatograph) until equilibrium between the headspace and water was reached following the procedure outlined in Wanninkhof and Thoning (1993) and Chipman et al. (1993). The overall internal precision of the $pCO_2(20)$ measurements for comparing the cruises was estimated at 4 μatm. Oxygen measurements were performed by the modified Winkler technique with most of the cruises in the 1990s and 2000s using automated colorimetric endpoint detection (Friederich et al., 1984). The precision of the O_2 measurements on each cruise was better than 1 μmol kg^{-1}, but between cruises the uncertainty was estimated at 3 μmol kg^{-1} due to differences in standardization and blank assessment.

3. Methodology

3.1. Data treatment

All data used in this study are served from the Carbon Dioxide Information and Analysis Center (CDIAC) and the CLIVAR and Carbon Hydrographic Data Office (CCHDO), and are archived at http://cdiac.ornl.gov/oceans/RepeatSections. The measurements were made following strict sampling and analysis protocols. The chemical data (O_2, DIC, pCO_2, and CFCs) were analyzed with similar instruments and often by the same groups for the different time periods, assuring consistency between measurements. Much of the data have been compared for consistency in previous papers (Wanninkhof et al., 2003; Lamb et al., 2002; van Heuven et al., 2011; Gruber et al., 1996; Gouretski and Jancke, 2001) and in community intercomparison exercises such as the Global Ocean Data Analysis Project, GLODAP (Key et al., 2004), Pacific Interior Carbon Data Synthesis, PACIFICA (Ishii et al., in press), and Carbon in the Atlantic, CARINA (Tanhua et al., 2010). Appendix B provides details on these data and the corrections applied. In short, no corrections were applied to the $pCO_2(20)$ data. Oxygen values were adjusted by 7.5 μmol kg^{-1} for the Ocean-Atmosphere Carbon Exchange Study, OACES (1993), and by a multiplicative factor of 0.98 for AJAX. A correction of 10.9 μmol kg^{-1} was applied to the DIC values, and a correction of 8 μmol kg^{-1} was applied to the TAlk values of AJAX (van Heuven et al., 2011). No TAlk measurements were performed during the SAVE and AJAX cruises, and no systematic offsets in corrected TAlk were observed within the uncertainty of ± 5 μmol kg^{-1} used as a cutoff.

For our analyses, only measurements with a quality control flag of 2 or 6, indicating a good or good duplicate measurement, were retained. All data used were gridded on a regular grid of 2° latitude by 100 m depth using a Kriging interpolation scheme and the contouring package Surfer™ (V6.0). The gridded products were subsequently subtracted to determine the temporal differences in concentration between the different time periods. The entire dataset from surface to bottom was gridded to minimize boundary artifacts, but the results are presented for depths below 2000 m. A comparison of the gridded data with the original data suggests no discernible gridding artifacts. Care was taken not to use any gridded output outside of the data domain for the interpretation.

CFC11 concentrations were used in the interpretation as an indicator of whether the water in the interior had been exposed to the atmosphere in recent times. Since CFC11 is a man-made compound not emitted into the atmosphere in appreciable quantities until the early 1950s, detection of CFC11 in deep water suggests, at least, partial ventilation of the water parcel since the 1950s. The concentration of CFC11 measured on the CLIVAR/CO_2 cruises was used rather than the difference between the occupations. The blank levels and uncertainties in the low concentrations in the deep water of the earlier cruises were significantly higher, sometimes leading to negative differences in the deep water. Of note is that by 1950 the atmospheric CO_2 level had increased by 30 ppm compared to pre-anthropogenic values of 280 ppm, or 25% of the current perturbation of ≈ 100 ppm. Thus, the absence of detectable CFCs in deep water does not preclude the presence of anthropogenic carbon.

The general characteristics of $pCO_2(20)$ and its values in different ocean basins are provided in Wanninkhof and Feely (1998) and summarized in Appendix A. The $pCO_2(20)$ parameter

Table 2
Representative deep-water values (≈ 3000 dbar) for the cruises used in this study and the sensitivity of $pCO_2(20)$ to changes in DIC and TAlk.

Cruise[a]	Lat.	Theta °C	Salinity °/oo	DIC μmol kg^{-1}	TAlk μmol kg^{-1}	$\partial pCO_2/\partial$TAlk μatm/μmol kg^{-1}	$\partial pCO_2/\partial$DIC μatm/μmol kg^{-1}	Re[b] $\partial pCO_2/pCO_2(\partial DIC/DIC)^{-1}$
A16N	24°N	2.50	34.94	2188	2341	−4.0	4.6	13.5
A16S	24°S	2.47	34.92	2180	2323	−4.5	5.0	13.9
A13.5	25°S	2.17	34.87	2200	2340	−4.6	5.2	14.0
P18	22°N	1.43	34.67	2357	2436	−8.4	9.2	16.3
P18S	24.5°S	1.60	34.68	2306	2403	−7.1	7.8	15.7

[a] A16N: Station 84, sample 108, 7/20/2003, 3000 dbar; A16S: Station 77, sample 110, 10/02/2005, 3098 dbar; A13.5: Station 59, sample 105, 3/29/2010, 3001 dbar; P18: Station 5, sample 101, 12/18/2007, 3112 dbar; P18S: Station 92, sample 104, 1/14/2008, 3033 dbar. Data from: http://cdiac.ornl.gov/oceans/RepeatSections/clivar_table_inv.html.
[b] Re = Revelle factor.

is a sensitive indicator of change in ocean carbon chemistry, but it is not a unique tracer of anthropogenic CO_2 since it is impacted by changes in TAlk and DIC. The TAlk parameter was not measured on all of the cruises or not measured with sufficient accuracy to quantify differences over time. The dissolution of calcium carbonate or the movement of water masses would cause a change in TAlk, but neither effect is anticipated to be large in the interior. As described in Appendix A, an increase in TAlk due to dissolution will cause a decrease in $pCO_2(20)$ but have a proportionally smaller impact than changes in DIC. Numerical models confirm invariant TAlk in deep water (Ilyina et al., 2009) and, for the analysis, we assume no changes in TAlk over the time periods. For the deep water, an increase in DIC will cause a large increase in $pCO_2(20)$ due to the decreased buffering capacity of the deep water compared to surface water.

The pCO_2 change with respect to DIC can be expressed in terms of the Revelle factor, Re (Takahashi et al., 1980), at TAlk, temperature (T), and salinity (S):

$$\mathrm{Re} = \left((\partial pCO_2/pCO_2)/(\partial \mathrm{DIC}/\mathrm{DIC})\right)_{\mathrm{TAlk},T,S} \quad (1)$$

with its inverse providing the buffer capacity. As shown in Table 2, the change in $pCO_2(20)$ ranges from 5 to 9 μatm per μmol kg^{-1} in DIC_{TAlk}, and from −4 to −8 μatm per μmol kg^{-1} in $TAlk_{DIC}$ for Re factors of 14 to 16 for the deep waters under investigation. While the inaccuracy of pCO_2 measurements is about twice that of DIC, the examples in Table 2 indicate a dynamic range of $pCO_2(20)$ that is five to nine times that of DIC. In other words, changes in $pCO_2(20)$ will manifest themselves above the analytical uncertainty before changes in DIC or TAlk.

We utilize this sensitivity to determine the change in DIC associated with the observed $pCO_2(20)$ change in deep water over the time intervals. The partial derivatives that make up the Re factor are discretized:

$$\Delta \mathrm{DIC}_{pCO_2} \approx \mathrm{DIC}(\Delta pCO_2/pCO_2)/\mathrm{Re} \quad (2)$$

where Re is computed using an inorganic equilibrium model from the measured DIC, TAlk, S, and T (Lewis and Wallace, 1998, as adapted by Pierrot et al., 2006).

Eq. (2) shows that the change ΔDIC_{pCO_2} is proportional to ΔpCO_2 and to the absolute values of DIC, $pCO_2(20)$, and Re. The greatest sensitivity will be to the change in pCO_2 over the time interval. An uncertainty analysis of ΔDIC_{pCO_2} based on the range of Re in deep water and the analytical uncertainty in DIC and pCO_2 is provided in the discussion section. The approximation is valid if the changes in deep water properties over time, other than pCO_2, are small. Moreover, the range in properties should be limited. The average, range, and standard deviation of T, S, DIC, $pCO_2(20)$, of the deep water sections for the two times of occupation are provided in Table 3. The range in values of discrete samples in the deep-water for the transects are about a tenth of that observed for the full water column and are very similar for the repeat occupations. Since the repeat transects did not sample the same locations or depths the close correspondence of average, range, and standard deviation over time suggests that representative samples are used in the gridding procedure used to quantify the changes.

Table 3
Minimum (Min), maximum (Max), and average (Av) values of deep water (> 2000 m) samples for A16, A13.5, and P18 for the different occupations.

	Pot. T	Salt	O_2	TAlk	DIC	$pCO_2(20)$	Re
A16 (60°N–56°S)							
2003/2005							
Av	1.8	34.84	237	2341	2209	839	13.8
StDev [a]	1.05	0.1	16	16	33	112	0.6
Count [b]	1067	1067	1067	1067	1067	466	466
Max	4.15	35.12	291	2375	2272	1097	15.3
Min	−0.5	34.66	190	2297	2155	549	11.4
1989/1993							
Av	2.08	34.88	241	2342	2200	812	
StDev [a]	0.99	0.1	14	16	29	102	
Count[b]	732	732	732	684	732	732	
Max	4.2	35.13	279	2400	2291	1088	
Min	−0.59	34.65	196	2302	2152	721	
A13.5 (10°S–55°S)							
2010							
Av	1.84	34.83	224	2347	2220	879	14.6
StDev [a]	0.68	0.07	11	12	21	95	0.6
Count [b]	795	795	768	754	756	694	690
Max	3.25	34.93	288	2386	2265	1141	15.7
Min	0.23	34.68	180	2269	2113	793	13.8
1983 (***AJAX***)							
Av	1.81	34.82	223	2348	2220	920	
StDev [a]	0.72	0.07	11	12	23	105	
Count[b]	574	574	564	79	87	96	
Max	3.15	34.93	243	2369	2251	1109	
Min	0.12	34.67	192	2320	2174	784	
P18 (20°N–45°S)							
2007							
Av	1.59	34.68	143	2414	2323	1234	15.9
StDev [a]	0.26	0.02	23	20	25	110	0.3
Count [b]	1024	1024	999	500	731	192	188
Max	2.28	34.71	195	2446	2366	1576	17
Min	0.82	34.58	82	2358	2271	1045	15.3
1994 (***CGC94***)							
Av	1.55	34.67	142	2412	2326	1216	
StDev[a]	0.26	0.02	23	20	27	107	
Count[b]	1250	1241	1206	303	313	336	
Max	2.27	34.72	196	2458	2367	1560	
Min	0.79	34.62	82	2354	2271	1047	

[a] Standard deviation of the measured values > 2000 m.
[b] Number of discrete samples analyzed for the particular parameter.

DIC can be corrected for changes in remineralization and respiration over time by assuming a Redfield stoichiometric relationship between carbon and oxygen (e.g. Anderson and Sarmiento, 1994). However, as shown in Figs. 2–4, changes in oxygen levels are

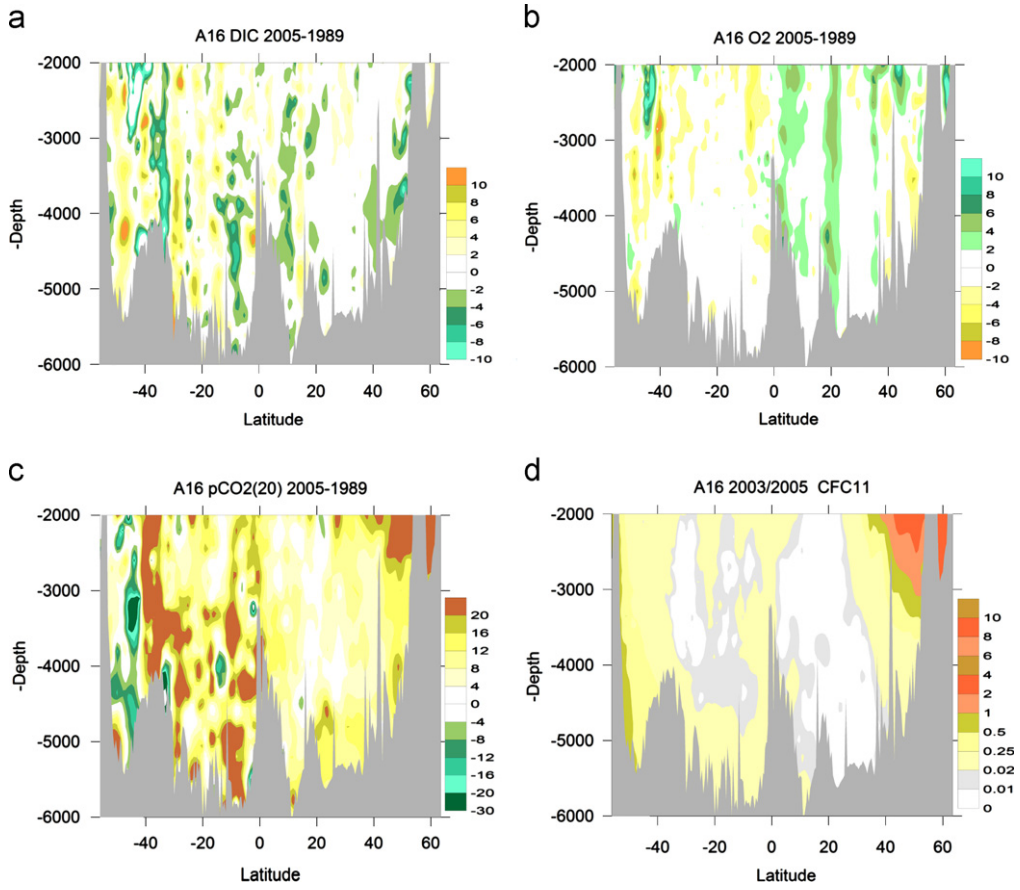

Fig. 2. Contour plots of differences in: (a) DIC in μmol kg^{-1}; (b) O_2 in μmol kg^{-1}; (c) the partial pressure of CO_2 measured at 20 °C ($pCO_2(20)$ in μatm) between 2005 and 1989 for the southern section and 2003 and 1993 for the northern section of the A16 line; and (d) CFC11 in pmol kg^{-1} for 2003 (north) and 2005 (south). The O_2 color bar is inverted to show the correspondence between increases in DIC and decreases in O_2 that are indicative of remineralization changes. The color scales have concentration differences blanked that are less than the analytical error of the measurements.

observed in the interior deep ocean but they are not systematic. Applying a remineralization correction to DIC values causes more small-scale variability compared to ΔDIC. This is attributed to uncertainties in the accuracy of the O_2 analyses for the different reoccupations. The assumption that natural DIC changes are directly proportional to O_2 according to a Redfield proportionality is not always valid (Wanninkhof et al., 2010). Therefore, no adjustments were made to ΔDIC for the observed changes in O_2.

The analysis is limited by the quality and quantity of support measurements needed to quantify and attribute changes in DIC. The following approximations and assumptions were made: there were no systematic changes in O_2 and TAlk in deep water for the cruises investigated, and the change in Re factor was assumed small. These assumptions do not have an appreciable impact on the large scale ΔDIC_{pCO_2}, whose magnitude is dominated by ΔpCO_2. The overall uncertainty for these assumptions and analytical uncertainty in the measurements are included in the error estimates.

3.2. Model output

The numerical model used in this study was the ocean component of the NCAR CESM1-BGC coupled with an ecosystem biogeochemistry model (Moore et al., 2004; Doney et al., 2009). The ocean physics model was from the Community Climate System Model (CCSM-4) (Gent et al., 2011). The simulations were forced in historical hindcast mode with physical climate forcing from atmospheric reanalysis and satellite data products (Doney et al., 1998, 2007) and prescribed historical atmospheric CO_2 and CFC11 levels. The model had a 0.5 to 1° resolution in the horizontal and about 60 layers with increasing thickness from 10 m at the surface, to 250 m from 3500 m to the bottom. The model resolution roughly corresponded to the sampling resolution of the cruises. The model runs were performed up to the year 2007. The model was subsampled along the hydrographic sections for the years the cruises took place, except for the A13.5 (2010) and P18 (2007/2008) cruises, for which the model results were linearly extrapolated to the appropriate year of the cruise. Since the model experienced numerical drift that could be misinterpreted as change over time, output from a control simulation with steady, pre-anthropogenic atmospheric CO_2 levels was subtracted from the output of the transient simulation forced with the observed increasing atmospheric CO_2 levels. This difference is the model-estimated anthropogenic CO_2 content in the ocean, C_{anthro}. The changes in C_{anthro} over time, ΔC_{anthro}, were compared to the measured ΔDIC and ΔDIC_{pCO_2}. The modeled and measured CFC11 concentrations were used to compare the penetration of the anthropogenic signal. The anthropogenic CO_2 uptake in the model was on the lower end of the model and observational approaches (Khatiwala et al., 2012).

4. Results

Cross sections that show the changes in the deep ocean for DIC, O_2, and $pCO_2(20)$ for the A16, A13.5, and P18 transects are provided in Figs. 2–4. The CFC data from the more recent occupations of the transects are also shown. Differences less than the stated analytical uncertainty are blanked in the figures. Each

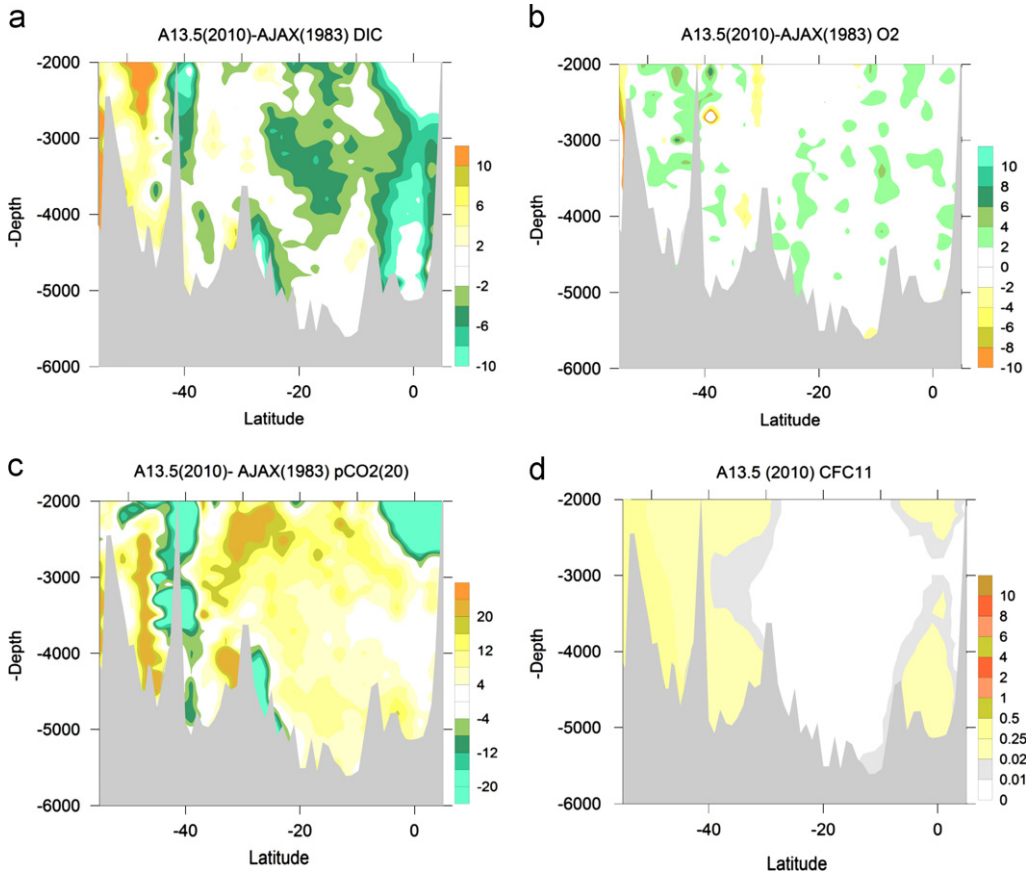

Fig. 3. Contour plots of differences in: (a) DIC in μmol kg^{-1}; (b) O_2 in μmol kg^{-1}; (c) the partial pressure of CO_2 measured at 20 °C ($pCO_2(20)$ in μatm) between 2010 and 1983 for the A13.5 line; and (d) CFC11 in pmol kg^{-1} for 2010. The O_2 color bar is inverted to show the correspondence between increases in DIC and decreases in O_2 that are indicative of remineralization changes. The color scales have concentration differences blanked that are less than the analytical error. Adjustments to the 1983 AJAX DIC and O_2 values have been applied as described in the text.

of the transects shows changes in DIC, O_2, and $pCO_2(20)$ at depth over the past one to three decades. Since the magnitude and spatial patterns of some of the changes are not consistent between biogeochemical parameters, it suggests systematic and random errors greater than the stated analytical precision. At high latitudes near the deep water formation regions, increases are clearly apparent in $pCO_2(20)$ and CFC11 for the A16 transect, and in CFC11 for the P18 transect, suggesting a penetration of anthropogenic signals. Changes in deep water temperatures are also observed (Purkey and Johnson, 2010). Of note is the vertical banded structure of the anomalies observed in our results and in the temperature anomalies. This has been attributed to changes in the location of fronts over time and mesoscale eddies or isopycnal heave that displace the isopycnals (Purkey and Johnson, 2010; Levine et al., 2008). The presence of measurable CFC11 in the deep water in each of the sections indicates anthropogenic penetration.

4.1. A16

The changes in DIC, O_2, and anthropogenic CO_2 between the occupations in the 1990s and 2000s along the A16 section are described in Wanninkhof et al. (2010). The A16 section crosses the Mid-Atlantic Ridge near the equator and traverses the western deep basins in the South Atlantic and the eastern deep basins in the North Atlantic. Aside from a clear anthropogenic CO_2 signal over the two decades that penetrates into the deep water (>2000 m) at high latitudes (see Fig. 4 in Wanninkhof et al., 2010), there are also differences attributed to analytical errors or natural variability as manifested by the changes in O_2 (Fig. 2). The DIC shows both small positive and negative anomalies that appear as vertically-coherent striations throughout the water column and sometimes are inversely related to O_2. Overall, the changes in deep water are close to the experimental uncertainty. Assuming an analytical accuracy of DIC of 2 μmol kg^{-1} for each cruise, the uncertainty in the differences is about 3 μmol kg^{-1}. Observed O_2 changes in deep water are also small and, like the DIC changes, are close to analytical accuracy, particularly since there is no absolute reference for O_2. The $pCO_2(20)$ values show a clear increase for most of the basin with generally larger changes in the south, partially attributed to the longer time period between the cruises (16 years in the south compared to 10 years in the north). Fig. 2 shows a large increase in $\Delta pCO_2(20)$ at 40 °S and a large decrease just south of this centered at 3500 m. This is a region with large $pCO_2(20)$ gradients (see Fig. A2, top panel), and the observed pattern could be caused by the movement of the subpolar front. However, there are no large corresponding changes in the other parameters. The increases in $\Delta pCO_2(20)$ are greater near the bottom (>4000 m) compared to the 2000–4000 m depth, which is caused by the deep circulation and is consistent with the deep ocean warming trends observed for the same section (Johnson and Doney, 2006). The CFC11 cross section below 2000 m for 2003/2005 shows CFC concentrations well above the instrumental and sampling blank values for much of the transect, indicating exposure of at least some of the deep water to the atmosphere in the last 60 years. Like the $pCO_2(20)$ section, the lowest CFC11 values are encountered in the

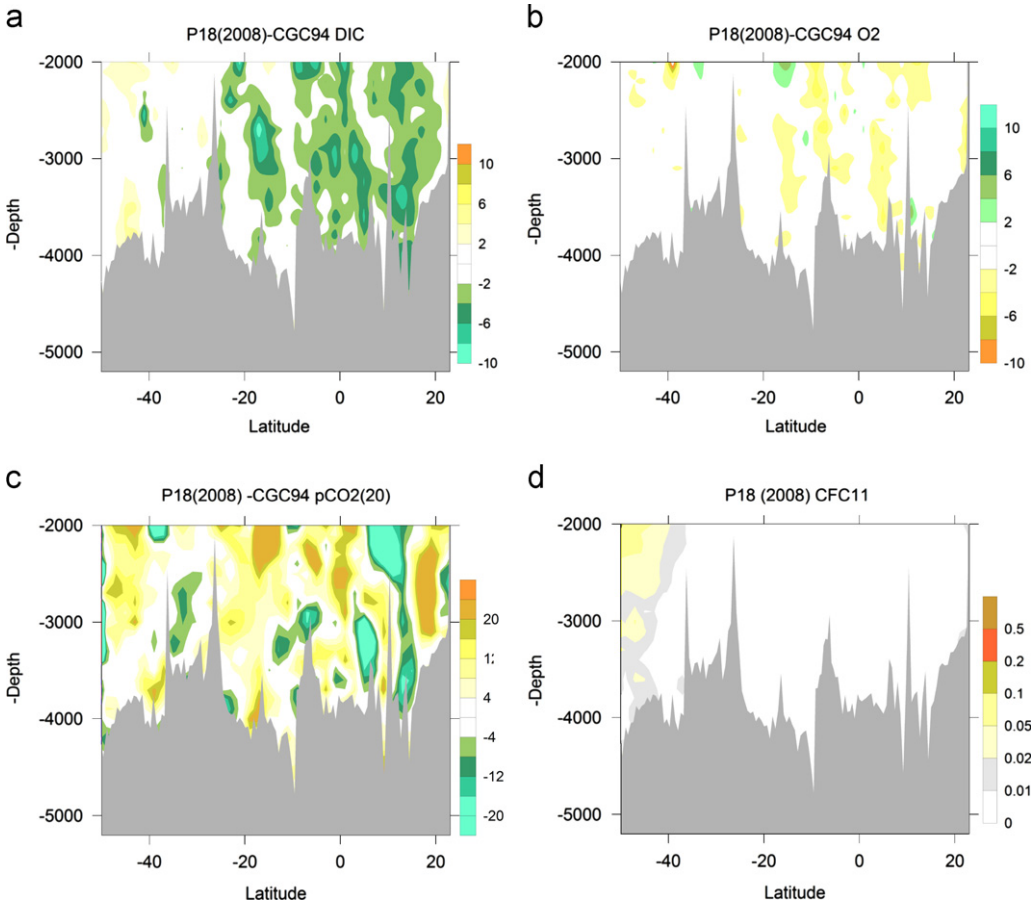

Fig. 4. Contour plots of differences in: (a) DIC in μmol kg^{-1}; (b) O_2 in μmol kg^{-1}; (c) the partial pressure of CO_2 measured at 20 °C ($pCO_2(20)$ in μatm) between 2008 and 1994 for the P18 line; and (d) CFC11 in pmol kg^{-1} for 2008. The O_2 color bar is inverted to show the correspondence between increases in DIC and decreases in O_2 that are indicative of remineralization changes. The color scales have concentration differences blanked that are less than the analytical error.

2000–4000 m depth range in the ocean interior rather than near the bottom.

4.2. A13.5

The A13.5 section sampled the deep eastern basins of the South Atlantic. Data coverage for $pCO_2(20)$ and DIC during the 1983 AJAX cruise was sparse, with only about 50 samples deeper than 2000 m between 25°S and 10°S and less than 10 samples between 10°S and 5°N such that significant interpolation errors are possible. Because of a lack of DIC and $pCO_2(20)$ data north of 10°S for AJAX, only the differences south of 10°S were determined. An additive correction of 10.9 μmol kg^{-1} was applied to all of the 1983 DIC data based on a comparison of the southern part of the line (van Heuven et al., 2011). However, Chipman et al. (1986) applied a trend correction to the DIC data such that a constant offset might not be appropriate. A multiplicative bias correction of 0.98 in O_2 was applied to the AJAX data and, with this correction, the difference between the occupations was small (Fig. 3b). Fig. B1 in Appendix B shows the differences in DIC and O_2 using the original uncorrected data. The $pCO_2(20)$ data show increases of between 4–16 μatm but with some notable decreases to the north and around Discovery Table Mount near 43°S. The CFC11 concentrations in 2005 showed large regions with measurable deep water CFC11 levels. The DIC changes at high latitudes are in areas with increases in CFC11. There is a correspondence between measurable CFC11 and changes in $pCO_2(20)$ at mid latitudes (20–35°S) with higher concentrations near the bottom compared to the 3000–4000 m depth range. This is attributed to the ventilation of bottom waters from the south. The A13.5 section also shows elevated CFC11 concentrations near the equator due to the transfer of younger, western deep water through the Romanche Fracture Zone near the equator (Mercier and Speer, 1998).

4.3. P18

The P18 section crosses the East Pacific Rise (EPR) near 5°S and traverses the deep basins to the west of the EPR in the North Pacific and to the east of the EPR in the South Pacific. The cruises extended from 23°N–67°S, but there are slight differences in the cruise tracks for the two time periods in the north and in the south. The P18 line shows apparent decreases in DIC in the northern part of the section between 1994 and 2008 (Fig. 4) and small increases to the south. The magnitude of decrease of 2–6 μmol kg^{-1} is not in agreement with O_2 patterns. Oxygen levels overall are unchanged, except that more areas appear with small decreases in O_2 in the northern region. The decreases in DIC and O_2 are likely due to small biases in the data between the time periods and, possibly, the movement of local fronts. The change in $pCO_2(20)$ is predominantly positive and in the 4–12 μatm range. There are also notable local negative anomalies that are not correlated with the other parameters. The CFC11 signal shows a clear ventilation pattern through Antarctic Bottom Water and Antarctic Intermediate Water in the south up to 40°S, but there is no strong signal further north, confirming the isolation of the water in the Chile and Peru basins of the South Pacific.

Table 4
Average specific inventory changes for DIC, DIC_{pCO_2}, and C_{anthro} in deep water (> 2000 m) and for the full water column for the A16, A13.5, and P18 lines (in mol m^{-2} yr^{-1}). The uncertainties are the standard deviation from the mean of the differences on the 2° interpolated grid.

Cruise	Latitude range	Time period	ΔDIC	ΔDIC_{pCO_2}	ΔC_{anthro} (model)
> 2000 m					
A16	63°N–56°S	1989 – 2005[a]	0.04 ± 0.42	0.47 ± 0.25	0.17 ± 0.25
A13.5	55°S–10°S	1983 – 2010[b]	−0.07 ± 0.38	0.12 ± 0.13	0.02 ± 0.01
P18	45°S–20°N	1994 – 2008	−0.25 ± 0.24	0.07 ± 0.12	0.00 ± 0.01
Full water column					
A16	63°N–56°S	1989 – 2005[a]	0.63 ± 0.95	*1.21 ± 0.74*[c]	0.75 ± 0.51
A13.5	55°S–10°S	1983 – 2010[b]	0.61 ± 0.94	*0.57 ± 0.35*[c]	0.47 ± 0.15
P18	45°S–20°N	1994 – 2008	0.41 ± 0.79	*0.88 ± 0.53*[c]	0.38 ± 0.24

[a] Measured concentration differences for the northern section (2°S–63°N) were for 10 years (1993–2003), while for the southern section it was 16 years. The specific inventory is on a per annum basis (in mol m^{-2} yr^{-1}).

[b] Lack of deep-water data from 10°S to 5°N during the 1983 AJAX cruise precludes quantitative estimates of change for this region. The ΔC_{anthro}(model) is for 1983–2007.

[c] Because of changing chemical characteristics in the upper water column, the assumptions of constant S, T, and TAlk used to calculate deep-water Re in Eq. (2) are not valid. The values are for illustrative purposes for comparison with ΔDIC_{pCO_2} > 2000 m.

5. Discussion

The A16, A13.5, and P18 transects are the only ones where decadal repeat observations of $pCO_2(20)$ have been made to date and therefore, together with DIC, O_2, and CFC11 measurements, make a unique dataset to study deep water CO_2 changes in the interior over time. The observed decadal signals are up to an order of magnitude smaller than in the upper water column. The issues of analytical precision and possible small biases in the analyses between the occupations cause an appreciable uncertainty in the observed changes. The DIC changes are not significant at these depths and, therefore, ΔDIC_{pCO_2} (Eq. (2)) is used. However, even with the greater response of ΔDIC_{pCO_2}, quantitative estimates of deep water increases in DIC are challenging, and the results are interpreted on a large scale. The range of uncertainty for the basin-wide average of DIC_{pCO_2} for A13.5 and P18 does not exclude 0, i.e., no change (Table 4).

Propagating errors of the quantities used in Eq. (2) can provide an estimate of the mathematical uncertainty ΔDIC_{pCO_2} of

$$\delta\Delta DIC_{pCO_2}/\Delta DIC_{pCO_2} = \delta DIC/DIC + [(\delta(\Delta pCO_2/pCO_2)/(\Delta pCO_2/pCO_2)] + \delta Re/Re \quad (3)$$

where δ is the uncertainity. Using δRe of 0.6 (Table 3), 3 μmol kg^{-1} for δDIC, and 5 for $\delta\Delta pCO_2/pCO_2$), along with the average values in Table 3, yields an error of ≈5% in $\delta\Delta DIC_{pCO_2}/\Delta DIC_{pCO_2}$. This excludes variability and unquantified uncertainties caused by instrument drifts and offsets between the cruises that increase the uncertainty in the results.

The method of estimating anthropogenic CO_2 changes from ΔDIC_{pCO_2} (Eq. (2)) is suited to the deep water of the interior ocean where water properties do not vary appreciably (Table 3) and isopycnals align with constant depth horizons. Using ΔDIC_{pCO_2} to determine inorganic carbon changes near the surface is problematic because of the large changes in Re and alkalinity, invalidating the assumptions. Therefore, there is limited opportunity to verify this approach with other means of estimating DIC changes over time, except for the North Atlantic.

For the A16 line, there is an appreciable change in anthropogenic CO_2 below 2000 m over the time span (Wanninkhof et al., 2010). A comparison of the extended multi-linear regression method, eMLR, as applied along isopycnal surfaces by Wanninkhof et al. (2010), and the ΔDIC_{pCO_2} method over isopycnal range σ_2=36.9–36.96, referred to as 36.95 from 45°N to 45°S, is provided in Fig. 5. Over this latitude range, the depth of this layer is at 1980 ± 148 dbar, except from 25–40°S where it deepens to 2400 dbar. The isopycnal shallows appreciably at higher northern and southern latitudes (Fig. 5). The change in DIC determined by the two methods, that is attributed to anthropogenic CO_2 increases, shows a similar pattern with a minimum at 15–20°N where the water mass ages are the greatest. To the north of this region, the ΔDIC increases rapidly for both methods. From 0° to 20°S, waters are ventilated from the west and show an appreciable change in DIC over the time period. At higher southern latitudes, the ΔDIC increases from ventilation and transport from southern outcrop regions. The σ_2=36.95 isopycnal shallows dramatically south of 45°S, and the assumptions of constant TAlk and Re of the ΔDIC_{pCO_2} method are not applicable.

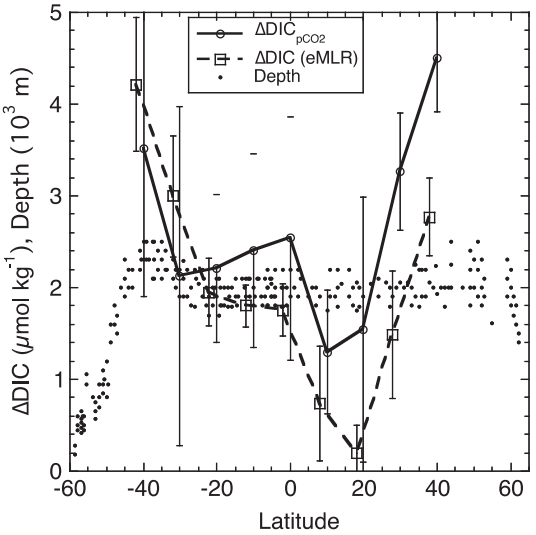

Fig. 5. Comparison of changes in CO_2 using the ΔDIC_{pCO_2} method (open circles and solid line) and the $eMLR_{dens}$ approach (open squares and dashed line) (after Wanninkhof et al., 2010) for A16 along σ_2=36.95 from 1989–2005. The error bars depict the standard deviations of the 10° averages. The results for the northern section (A16N) are scaled linearly from 10 to 16 years to correspond with the southern section. The small solid squares indicate the depth range of the isopycnal interval (in 10^3 m).

Besides overall agreement, there are also differences between the results. There is less latitudinal variation observed in the ΔDIC_{pCO_2} method, and its uncertainty, as reflected in the standard deviation in the 10-degree averages, is greater than the eMLR approach that, by nature, includes significant smoothing. For the ΔDIC_{pCO_2} approach, the change over the decade is higher to the north than to the south, which is opposite to the eMLR approach along this isopycnal. In this respect, the ΔDIC_{pCO_2} is in agreement

with the numerical models and transient tracer-based approaches that show larger changes in the North Atlantic (Khatiwala et al., 2012).

To provide support that the observed changes in DIC in deep water are of anthropogenic origin, CFC11 data from the CLIVAR/CO_2 reoccupations were used as a qualitative indicator to determine if a component of the deep water was exposed to the surface during the past 60 years. The model output was used to aid the interpretation.

The anthropogenic CO_2 and CFC signals enter at the surface, and much of their signals reside in the upper 2000 m. This is illustrated in Fig. 6a and b for the A16 line where the normalized concentrations of CFC11, ΔC_{anthro}, ΔDIC, and ΔDIC_{pCO_2} are plotted versus depth. The Δ notation depicts the change over the time period between cruises: ΔDIC refers to the change in measured DIC values, and ΔDIC_{pCO_2} is based on the DIC change computed from pCO_2 changes (Eq. (2)). The ΔC_{anthro} refers to the change in modeled anthropogenic CO_2 over the time period between occupations. For the A16 section from 56°S to 63°N, the following percentages of the total water column burden are below 2000 m: 17% of the CFC11; 25% of the CFC11 in the model; 17% of the ΔDIC; 53% of the ΔDIC_{pCO_2}; and 25% of the ΔC_{anthro}(model). For CFC, these are the water column values for 2005, while for ΔDIC and ΔC_{anthro}(model) these values are for the change between 1989 and 2005. The ΔDIC_{pCO_2} estimates suggest an appreciably greater change in the deep water than based on DIC data. The model-based results show a close correspondence between CFC11 in the deep water and changes in C_{anthro} over the 16 years, with magnitudes of the C_{anthro} increase between those based on ΔDIC and ΔDIC_{pCO_2}. The ΔDIC shows greater variability with depth than ΔDIC_{pCO_2} despite basin-wide averaging (Figs. 6b and 7), likely due to the uncertainty in the small signal.

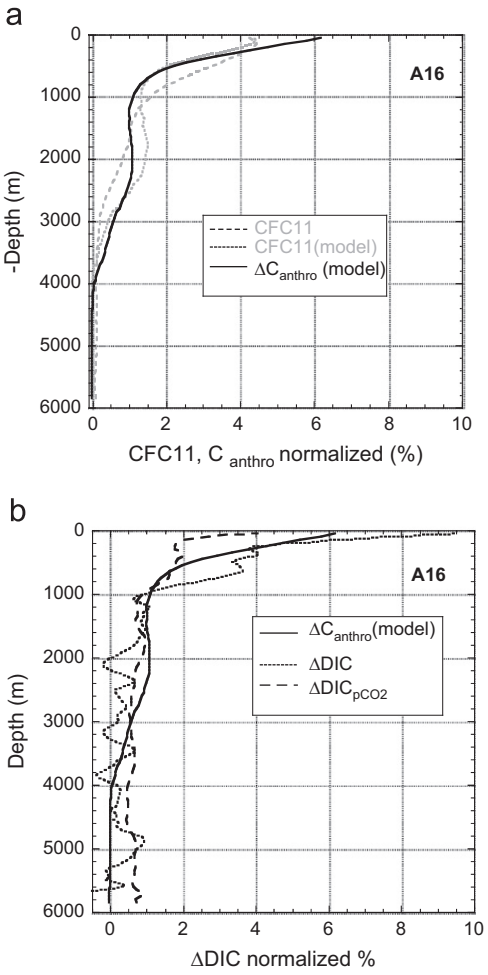

Fig. 6. Average normalized concentration profiles for A16 from 63°N to 56°S. The normalization is performed by taking the average concentration in each 50-m gridded depth interval and dividing it by the total water column inventory. Panel a shows the normalized concentrations of CFC11 and CFC11 (model) for 2005 and the modeled ΔC_{anthro} difference between 2005 and 1989. It shows higher CFC11 model concentrations at mid-depths than the CFC11 observations and an absence of CFC11 in the model but measured CFC11 below 4000 m. Panel b shows ΔC_{anthro}(model), ΔDIC, and ΔDIC_{pCO_2} for the time period from 1989–2005 with ΔC_{anthro}(model) going to zero below 4000 m but measurable changes in ΔDIC and ΔDIC_{pCO_2}. The ΔDIC_{pCO_2} shows relatively constant values below 1000 m.

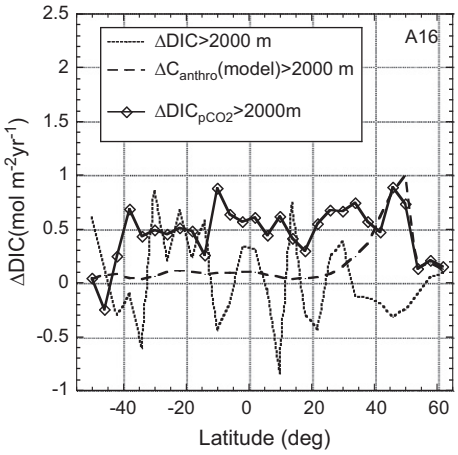

Fig. 7. Specific inventory changes of ΔDIC, ΔDIC_{pCO_2}, and ΔC_{anthro} (model) between 1989 and 2005 below 2000 m versus latitude for the A16 line.

The vertical water-column integrals, or specific inventory changes of ΔDIC, $\Delta pCO_2(20)$, and modeled ΔC_{anthro} versus latitudes below 2000 m for A16 are shown in Fig. 7, while measured and modeled CFC11 levels for 2003/2005 are provided in Fig. 8. For the Atlantic A16 section, there is a measurable signal in CFC11 below 2000 m for much of the section, reflecting the ventilated nature of the deep western and eastern Atlantic basins. The ΔC_{anthro}(model) results show anthropogenic CO_2 concentration changes over the 16 years that are less than 0.1 mol m^{-2} yr^{-1}, except for the high northern latitudes where changes of up to 1 mol m^{-2} yr^{-1} in the specific inventory are observed. The measured ΔDIC values show both positive and negative deviations from zero even at the high northern latitudes, and correction for remineralization using O_2 changes does not decrease the variability. The ΔDIC_{pCO_2} has relative constant levels of 0.6 mol m^{-2} yr^{-1} throughout the transect.

This lack of bigger changes in ΔDIC_{pCO_2} specific inventory at high northern latitudes is attributed to several factors. The observed penetration of anthropogenic CO_2 at the high northern latitudes appears lower than the model estimates for 1993 to 2003 (Wanninkhof et al., 2010) and is attributed to decreased ventilation in the mid-1990s (Pérez et al., 2010). This is supported by decreasing O_2 levels below $\approx$2500 m in the region (Fig. 2b). The shallow bathymetry of the Rockall Plateau also contributes to the smaller column inventory change $>$2000 m. The average inventory increase for the full transect from 54°S to 63°N for ΔDIC, ΔDIC_{pCO_2}, and modeled ΔC_{anthro} are given in Table 4. All of the methods show an appreciable increase in the deep water with ΔDIC_{pCO_2} showing the largest change.

The specific inventory of CFC11 measured during the A16 cruises in 2003/2005 is compared to the modeled CFC to assess if the ΔDIC_{pCO_2} can be attributed to anthropogenic CO_2 changes over the time interval. The modeled CFC inventory at depths greater than 2000 m is up to three times higher than measured at 50°N and remains higher to 20°N, after which it drops below the

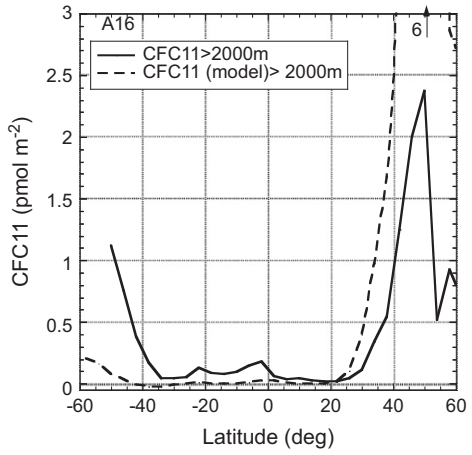

Fig. 8. Specific inventory for measured CFC11 and modeled CFC11 greater than 2000 m for 2003/2005 for the A16 line.

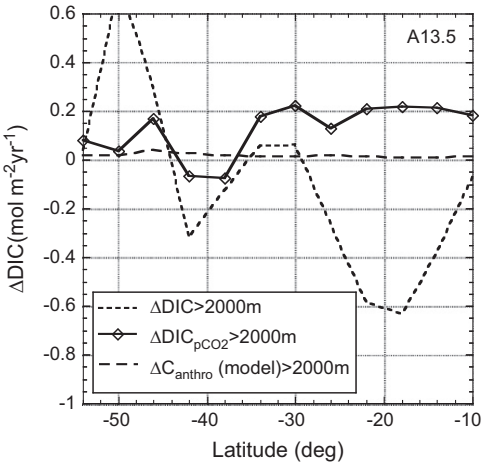

Fig. 9. Specific inventory changes of ΔDIC, ΔDIC_{pCO_2}, and ΔC_{anthro}(model) below 2000 m versus latitude for the A13.5 line from 54°S to 10°S between 1983 and 2010.

measured values. At latitudes greater than 30°S, a significant increase in the measured specific CFC inventory is observed compared to the model at depths greater than 2000 m (Fig. 8). This suggests that the penetration of CFC from the south in the model is sluggish and that the interior ocean in the model is less well ventilated than observations indicate (Doney and Hecht, 2002). The measurable CFC11 inventory at depths greater than 2000 m strongly suggests that C_{anthro} is present in much of the Atlantic interior. At first glance, the average A16 deep water ΔDIC_{pCO_2} inventory rate of change of 0.47 mol m^{-2} yr^{-1} (Table 4) seems high in light of the current global ocean average anthropogenic CO_2 uptake of $\approx$0.5 mol m^{-2} yr^{-1}. However, much of the deep Atlantic has CFC11 concentrations ranging from 0.1 to 0.4 pmol kg^{-1} that translates into a CFC age of 40–50 years or a water mass exposure in the 1960s. Khatiwala et al. (2009, 2012) show a global anthropogenic uptake of $\approx$0.3 mol m^{-2} yr^{-1} during this era which, considering the negative bias of CFC age compared to the water mass age for deeper waters, suggests that the change in specific inventory based on ΔDIC_{pCO_2} of 0.47 mol m^{-2} yr^{-1} is reasonable.

The A13.5 line is in a less ventilated region in the eastern basin of the Atlantic, with much of the anthropogenic signal coming from the south. However, CFCs indicate a northern source as well, originating from water in the western basin passing through the Romanche Fracture Zone. The inventory change below 2000 m in ΔDIC and ΔDIC_{pCO_2} and the ΔC_{anthro}(model) between 55°S and 10°S is shown in Fig. 9. The ΔDIC shows positive values > 44 °S but negative values further north, reflecting the uncertainty in the adjustment of the AJAX DIC values. The measured deep-water CFC11 inventory is appreciably higher than the modeled inventory (Fig. 10). The ΔDIC_{pCO_2} inventory also shows consistently higher values than the modeled ΔC_{anthro} inventory over the time period. The CFC11 data suggest that the model does not carry the anthropogenic CO_2 signal to depth on the same time scales as the observations suggest. The average, deep-water specific inventories for the transect (55°S to 10°S) show a six-fold greater inventory change for ΔDIC_{pCO_2} as for the modeled ΔC_{anthro} (Table 4). The nearly invariant S, O_2, and T at depth, and the presence of measurable CFC11 below 2000 m, suggest that the ΔDIC_{pCO_2} can be attributed to anthropogenic CO_2.

The average A13.5 deep-water ΔDIC_{pCO_2} inventory change is about 0.12 mol m^{-2} yr^{-1} and is six-fold greater than the C_{anthro} (model) inventory change from 1983 to 2010. The specific inventory change is a quarter of that determined for the A16 transect (Table 4). The measured CFC inventories in 2010 below 2000 m are lower than for A16 as well, as seen by comparing

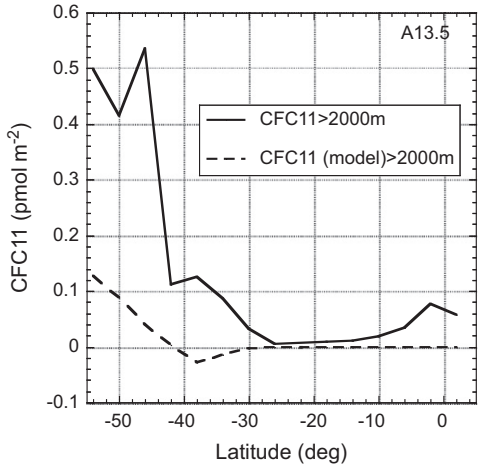

Fig. 10. Specific inventory for measured CFC11 and modeled CFC11 greater than 2000 m for 2010 for the A13.5 line.

Fig. 10 with Fig. 8. Of note is the lack of a clear increase in DIC towards the southern end of the A13.5 line, both in the C_{anthro} model and ΔDIC_{pCO_2} (Fig. 9) over the time period, while the CFC11 observational data for 2010 (Fig. 10) show a significant signal. The model shows a smaller deep-water CFC11 signal than the observations, consistent with the results of the A16 line, probably because of sluggish deep ventilation from the south in the model. The ΔDIC_{pCO_2} inventory at the southern end of the section is not expected to show as large a relative change as CFC because of the 10-fold smaller characteristic exchange time of gas fluxes for CFC compared to CO_2 and the relative small area of outcropping where the ventilation with the atmosphere takes place in the Southern Ocean (Sloyan and Rintoul, 2001). Low C_{anthro} inventories have been determined by other methods in the Southern Ocean (> 45 °S) (Sabine et al., 2004; Khatiwala et al., 2009) in agreement with our inventory change along A13.5 over the 27 years and with the ΔDIC_{pCO_2} from the A16 line at high southern latitudes.

The P18 line in the eastern Pacific has ventilated water at the southern end of the section and old water masses to the north. Modeled and measured CFC specific inventories for 2008 at depths greater than 2000 m plotted versus latitude show high inventories in the south, peaking between 60 and 50°S,

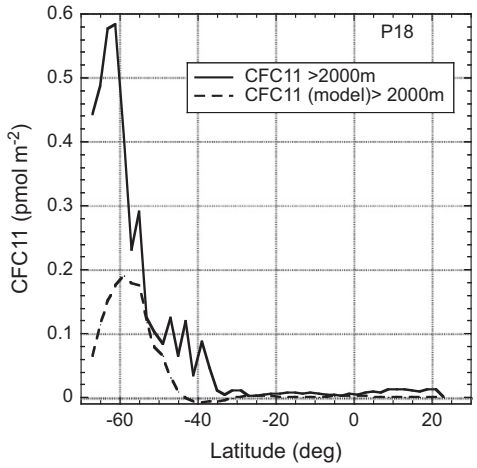

Fig. 11. Specific inventory for measured CFC11 and modeled CFC11 greater than 2000 m for the P18 line for 2008.

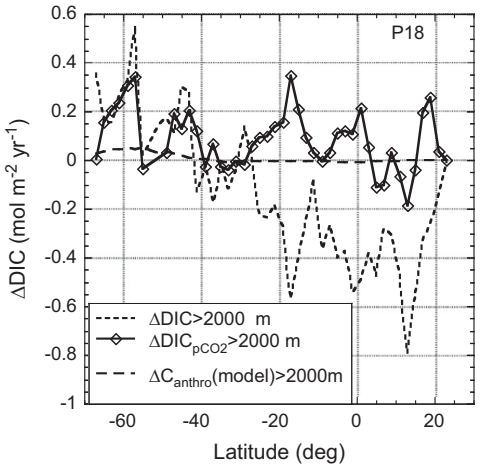

Fig. 12. Specific inventory changes of ΔDIC, ΔDIC_{pCO_2}, and ΔC_{anthro}(model) below 2000 m versus latitude for the P18 line between 1994 and 2008.

and very low values in the north (Fig. 11). The measured values are consistently greater. North of 30°S, the modeled inventories show no CFC11 below 2000 m, while the observations indicate low but measureable levels (≈ 0.01 pmol kg^{-1} m^{-2}), except near 25°S where both the model and observations indicate an absence of CFC11. Below 2000 m, the model section only shows C_{anthro} south of 40°S. Fig. 12 shows the ΔDIC with a decreasing northward trend ranging from 0.2 mol m^{-2} yr^{-1} in the south to -0.4 mol m^{-2} yr^{-1} in the north that suggests a spatial bias in the measurements similar to the observations along the A13.5 line. This can also be seen in Fig. 4a where the northern section has lower DIC values in the deep water for the more recent occupation. The biases in the specific inventory are within the DIC measurement error. The ΔDIC_{pCO_2} shows a small but overall positive inventory for the entire transect, averaging about 0.07 mol m^{-2} yr^{-1} (Table 4). For the full water column, the ΔDIC is similar to the modeled C_{anthro}, while ΔDIC_{pCO_2} is appreciably higher. The trends versus latitude show slightly elevated values in C_{anthro}(model) to the south but not to the extent of CFC11. As with the other transects, the latitudinal trend of ΔDIC_{pCO_2} is relatively flat. The magnitude of ΔDIC_{pCO_2} in the deep water is smaller than observed in the Atlantic in accord with the older water masses. The small magnitude and uncertainty in change in ΔDIC_{pCO_2} for the deep water does not exclude 0 (i.e., no change).

6. Conclusions

Decadal changes of inorganic carbon in the deep water of the ocean interior cannot currently be determined with confidence based on DIC measurements. Systematic changes in DIC and O_2 are observed that are beyond the stated analytical precisions, suggesting that additional factors such as biases during and between cruises, impact long-term comparisons of the measurements. The DIC changes based on discrete $pCO_2(20)$ measurements, ΔDIC_{pCO_2}, show inventory changes that are in general agreement with the age of the water masses and other indicators. Cruises in the South Atlantic western basin and North Atlantic eastern basin suggest rates of change in the deep water (>2000 m) DIC inventory of 0.47 mol m^{-2} yr^{-1}. The corresponding rates of change for the eastern South Atlantic deep basin are 0.12 mol m^{-2} yr^{-1} and for the eastern South Pacific 0.07 mol m^{-2} yr^{-1}. These changes are appreciably higher than the C_{anthro} output of the NCAR CESM1-BGC model, but this model also shows less CFC11 at depth than measured. The ΔDIC_{pCO_2} changes are plausible and of anthropogenic origin based on CFC measurements. The results indicate that appreciably more C_{anthro} is entering the ocean interior than several current observation- and model-based techniques indicate. The paucity in $pCO_2(20)$ data and appreciable uncertainty make the quantification of this signal tentative, particularly for the A13.5 and P18 lines where the change in $pCO_2(20)$ is small. As the anthropogenic CO_2 signal continues to rise in the deep ocean over time, there is strong merit in measuring $pCO_2(20)$, in addition to DIC and TAlk, during repeat hydrography cruises as sensitive indicators of change in the inorganic carbon cycle.

Acknowledgments

The ability to discern small changes in the deep ocean over decades is testament to the care and dedication of the many seagoing analysts that have performed the measurements and the personnel involved in quality control and data management. David W. Chipman has provided significant contributions to the development of shipboard measurements of pCO_2 used by the LDEO and AOML groups that are the cornerstone of this work. We appreciate the substantive and detailed comments of three reviewers that aided in improving the document. Ms. Gail Derr of AOML is gratefully acknowledged for providing extensive copy and style editing. We thank M. Long, K. Lindsay, and I. Lima for helping with the generation and analysis of the CESM-1 ocean-ice model results. Rik Wanninkhof, Geun-Ha Park, John L. Bullister, and Richard A. Feely appreciate the support from the NOAA Office of Atmospheric and Oceanic Research and the Climate Observation Division. S.C.D. acknowledges support from NOAA Grant NA07OAR4310098. T.T. has been supported by grants from NSF and NOAA. This is PMEL contribution 3847.

Appendix A. Discrete pCO_2 analyzed at a constant temperature of 20 °C ($pCO_2(20)$) and other inorganic carbon system parameters

The inorganic carbon system is generally described in terms of four parameters: total dissolved inorganic carbon (DIC); total alkalinity (TAlk); the partial pressure of CO_2 (pCO_2); and pH. The partial pressure of CO_2 is sometimes expressed as fugacity (fCO_2) that takes

into account the non-ideality of the gas (Weiss, 1974). Other abbreviations for DIC include TCO_2 and C_T. Total alkalinity is also abbreviated as A_T and TA. The DIC and TAlk are state variables that do not depend on temperature and pressure. They are core parameters for most surveys focused on the inorganic carbon cycle. There have been significant improvements in pH measurements and, in particular, spectrophotometric determination of pH has extreme precision. Advances in dyes and reference materials have greatly improved the accuracy of pH measurements. The pH can be expressed on different scales, e.g., the National Bureau of Standards scale (NBS), the total scale, the seawater scale, and the free scale. For oceanographic applications, the total and seawater scales are mostly used with a reasonably well-defined conversion routine between them. Recent recommendations are to report the pH of seawater on the free scale (Marion et al., 2011). The discrete pCO_2 and discrete pH measurements have many commonalities as parameters for constraining the inorganic carbon system and for detecting change (McElligott et al., 1998). They show a tight anti-correlation as can be seen in Fig. A1 where the pH at 25 °C on the seawater scale $pH_{sw}(25)$ and $pCO_2(20)$ are plotted for the P18 and A16S transects used in this study. The $pCO_2(20)$ and $pH_{sw}(25)$ parameters have a large signal to noise, facilitating the detection of small changes. Changes over decadal time scales for the ocean surface and intermediate depths have been obtained from discrete pH observations measured at constant temperature (Byrne et al., 2010).

Discrete pCO_2 has only been used by a few investigators for large-scale surveys (Neill et al., 1997; Wanninkhof and Feely, 1998), largely because of the relative complexity of the measurements and low sample throughput. It shares the benefits of pH measurements of very good precision. It has a strong temperature dependence and requires good temperature control and an accurate temperature for analysis. Measuring pCO_2 at a constant temperature has two important advantages over in situ measurements. It can provide a greater dynamic range of measurement if the temperature is raised from ambient. Secondly, at constant temperature, pCO_2 becomes a quasi-state variable by eliminating the temperature dependence of the parameter. Transects of $pCO_2(20)$ for the A16, P18, and A13.5 lines are provided in Fig. A2. These figures illustrate the wide dynamic range and appreciable differences in pCO_2 for these areas. The older, less ventilated regions such as P18 show significantly higher pCO_2 concentrations than the better ventilated region where A16 took place.

For the purpose of detecting changes in deep-water, $pCO_2(20)$ is a very sensitive indicator of change in DIC and is less affected by changes in TAlk. It is therefore a good tracer of anthropogenic CO_2. This is illustrated in Fig. A3, where the impact of changing DIC on $pCO_2(20)$ under C_{anthro} addition, organic matter dissolution, and carbonate dissolution scenarios is illustrated for A13.5 at $\approx$3000 dbar (see Table 2). Increases in DIC due to anthropogenic CO_2 input, or the remineralization of organic matter (soft tissue), with no appreciable change in TAlk will cause a large increase in $pCO_2(20)$. Changes in TAlk due to the dissolution of calcium carbonate will decrease the $pCO_2(20)$, but the magnitude of decrease is reduced because dissolution will also increase the DIC. The change in $pCO_2(20)$ due to dissolution is further mitigated, as it generally is accompanied by the oxidation of organic matter. In the example in Fig. A3, an organic to inorganic dissolution ratio of 1:1.5 leads to a nearly invariant $pCO_2(20)$. The plot also shows the DIC and corresponding $pCO_2(20)$ values for the deep-water values of the northern and southern locations of the P18 line (Table 3). If we assume a general water transport from the South Atlantic to the South Pacific and remineralization of organic material along its way, the $pCO_2(20)$ values fall well below the organic remineralization line. This is partially due to multi-endmember, non-linear mixing processes but also indicative that TAlk increases offset the impact of DIC increases on

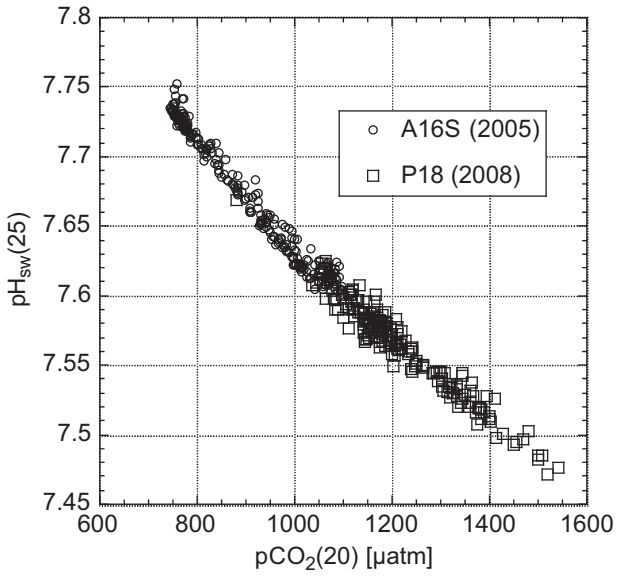

Fig. A1. Anti-correlation of $pCO_2(20)$ and $pH_{sw}(25)$ for depths > 2000 dbar for the P18 cruise in 2007/2008 and the A16 cruises in 2003 and 2005. $pH_{sw}(25)$ measurements were performed by the group of Prof. Millero at the University of Miami.

$pCO_2(20)$ from remineralization processes in the deep ocean. Thus, while we cannot definitively rule out changes in deep-water TAlk due to measurement imprecision, any changes would have a small impact on $pCO_2(20)$.

For the analyses presented, the pCO_2 is measured at 20 °C, while the temperature at depth ranges from about −0.5 to 4.15 °C (Table 3). Raising the temperature of the water samples to 20 °C causes a doubling of pCO_2 to levels of 700–2000 µatm (Fig. A2) and increases the dynamic range of measurement. This yields higher pCO_2 than in the ambient atmosphere, leading to the possibility of outgassing of the sample prior to and during analysis. Moreover, instruments need to be calibrated for high pCO_2 in a range where calibration gases are not readily available. For our studies, custom prepared calibration gases up to 1500 ppm in air and traceable to primary standards.

The merits of the $pCO_2(20)$ parameter include its sensitivity of change, insensitivity to temperature, and near-conservative behavior with respect to mixing, unlike pCO_2(in situ). It can, therefore, serve as a sensitive indicator of deep-water changes. As described in the text, the attribution of changes in deep water requires assumptions of constancy in other parameters such as TAlk and O_2 that cannot be resolved to the same sensitivity. As there are no seawater standards available for $pCO_2(20)$, the accuracy of the measurements can only be estimated from internal consistency measurements in which two of the four inorganic carbon system measurements are used to calculate the other two. This method does not provide an absolute accuracy estimate, as it is dependent on the dissociation constants used and the assumption of the contributions of other acids and bases to total alkalinity. To overcome the limitation of possible biases in the data, this study exclusively used data from the authors of this paper that used similar approaches, i.e., whose gas standards are traceable to the same primary reference and whose values are similar in cross-over analyses (Lamb et al., 2002).

Appendix B. Data used and corrections applied

For this study, the long-term accuracy and precision of data are of critical importance. Several global synthesis exercises have

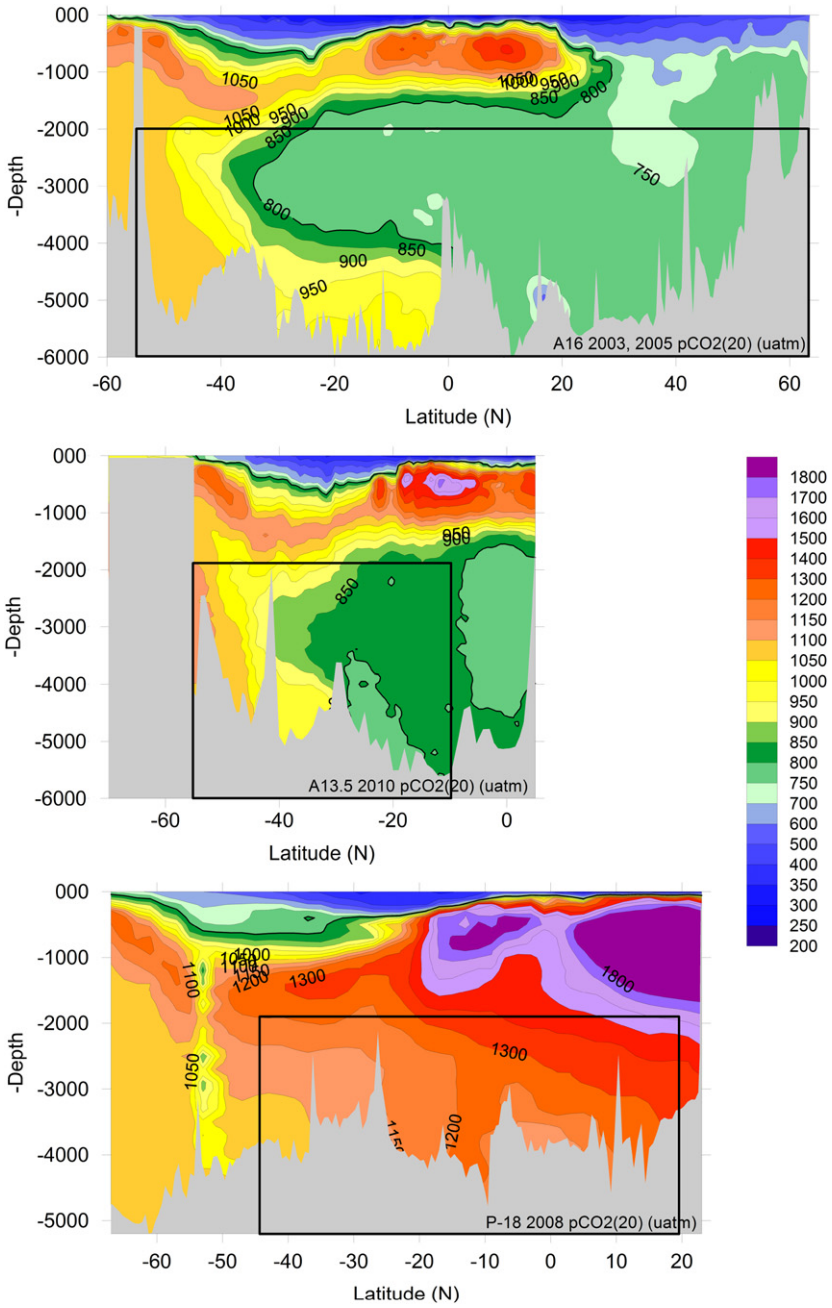

Fig. A2. Cross sections of $pCO_2(20)$ in μatm for the A16 transect occupied in 2003/2005 (top); the A13.5 transect occupied in 2010 (middle); and the P18 transect occupied in 2007/2008 (bottom). The rectangle in each figure shows the region in the deep water where the analyses were performed.

looked closely at the datasets and recommended adjustments to different biogeochemical parameters based on contextual data intercomparison. These include comparing deep-water data assuming no change in properties over time, and large-scale multiple regression techniques. An *a priori* assumption in these adjustment approaches is the constancy of values below 2000 m for the cruises compared. The efforts performed under the Global Ocean Data Analysis Project, GLODAP (Key et al., 2004), Carbon in the Atlantic Ocean, CARINA (Tanhua et al., 2010), and Pacific Interior Carbon Data Synthesis, PACIFA (Ishii et al., in press) have been invaluable in assuring mutual consistency between the cruises. The cruise data used in the analysis of deep-water CO_2 changes were checked against the adjustments proposed in the global and regional syntheses, taking care not to make adjustments that would impact our results by normalizing deep-water data over longer time periods (see Table B1).

When using the results for the syntheses to assess offsets and accuracy, the following points were considered:

- The A16, A13.5, and P18 cruises conducted in the 2000s were considered core cruises in the large scale syntheses and carried a greater weight in that the data from the onset were considered "good."
- The older cruises were conducted with appreciably less quality control procedures in place, and overall quality is not as good.
- The adjustments relied heavily on cruises intersecting each other.
- The adjustments were performed for the entire cruise and cannot account for trends in data that occur throughout a cruise.

Except for an Atlantic basin analysis of WOCE cruises by Wanninkhof et al. (2003) and a Pacific analysis in Lamb et al.

(2002), the $pCO_2(20)$ data have not undergone independent quality checks. The number of cruises with $pCO_2(20)$ was insufficient to perform contextual comparisons in the large syntheses activities. Chen et al. (1995) compared $pCO_2(20)$ data obtained by the groups of Takahashi and Wanninkhof from several cruises and did not discern any systematic biases between the cruises. Because of the consistency of data between the groups, we used these $pCO_2(20)$ data exclusively for our effort.

The oldest cruise used in this work is AJAX, and several of the parameters from the cruise have appreciable recommended corrections (see Table B1). The cruise was not included in the GLODAP effort, but the AJAX data have different recommended corrections in later exercises. An adjustment for TAlk of 0 μmol kg^{-1} was recommended in the CARINA effort by Hoppema et al. (2009) and 8 μmol kg^{-1} by van Heuven et al. (2011). Both efforts failed to specify that the TAlk parameter was calculated from $pCO_2(20)$ and DIC. We adopted the recommended adjustments from Table 3 in van Heuven et al. (2011). The similar magnitude adjustments in DIC (+11) and calculated TAlk (+8), calculated from $pCO_2(20)$ and DIC, indicate that the $pCO_2(20)$ measurements are consistent. Fig. B1 provides the differences in DIC and O_2 between 2010 and 1983 without corrections from Table B1 applied, which can be compared with Fig. 3 in the text where the corrected data are used. As described in the cruise documentation, http://cchdo.ucsd.edu/data/co2clivar/atlantic/ajax/ ajax_316N19831007do.txt, there appears to be spatial trends in the DIC data obtained on the cruise. The corrections in van Heuven et al. (2011) are based on the southern end of AJAX, and there is a suggestion in the cross section of DIC differences in

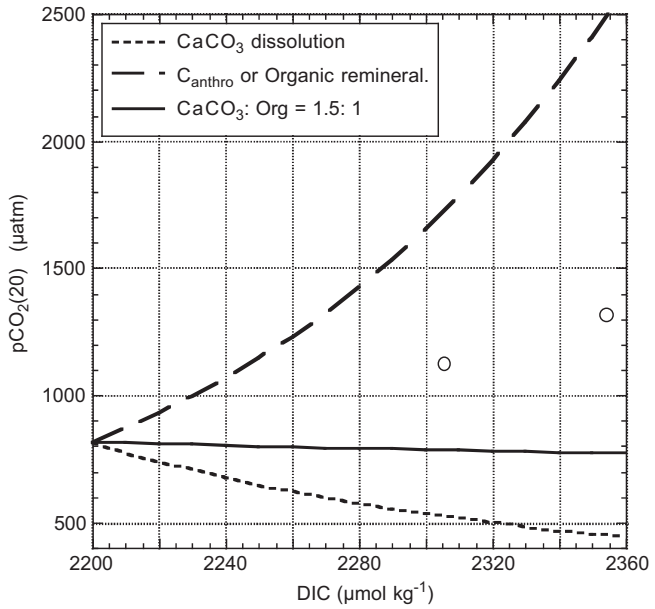

Fig. A3. Impact of the dissolution of carbonate and the addition of C_{anthro} or remineralization of organic material on $pCO_2(20)$. The initial values are representative of samples taken on A13.5 at ≈3000 dbar with T=2.2 °C; S=34.9; DIC=2200 μmol kg^{-1}; TAlk=2340 μmol kg^{-1}; PO_4=1.6 μmol kg^{-1}; NO_3=23 μmol kg^{-1}; and pCO_2=815 μatm. All scenarios were calculated using the CO2SYS program (Lewis and Wallace, 1998; Pierrot et al., 2006). For the dissolution of $CaCO_3$ (dotted line), a change of 1 μmol kg^{-1} in DIC yields a change of 2 μmol kg^{-1} in TAlk. For the addition of anthropogenic CO_2 (dashed line), there is no change in TAlk; for organic carbon remineralization there is a small decrease in alkalinity but it yields graphically indistinguishable results from the C_{anthro} addition (dashed line). The solid line is a scenario of a ratio of $CaCO_3$ dissolution to organic carbon remineralization of 1.5 to 1. The open circles are the deep water $pCO_2(20)$ and DIC levels at 25°S and 20°N on P18 with TAlk values of 2403 and 2436 μmol kg^{-1}, respectively.

Table B1
Adjustments to parameters used in our analysis.

Cruise	Adjustment (Source)			
	DIC	TAlk	$pCO_2(20)$	O_2
A16				
SAVE (1989)	NA(1)	NA(1)[a]	NA(1)	NA(1)
OACES (1993)	NA(2)	NA(2)	NA(2)	+7.5 (5)
A16N (2003)	NA(7)	NA(7)	NR	NA(7)
A16S (2005)	NA(7)	NA(7)	NR	NA(7)
P18				
CGC-94	NA(3)	NA(3)	NA(3)	x1.02(3)
P18 (2007)	NA(6)	NA(6)	NA(6)	NA(6)
A13.5				
AJAX	+10.9(4)	+8(4)[a]		x0.98(4)
A13.5(2010)	NR	NR		NR

NA: None applied.
NR: Not reported, but inspection during this effort does not suggest any offsets in the data.
(1) Key et al. (2004).
(2) Wanninkhof et al. (2003).
(3) Lamb et al. (2002).
(4) van Heuven et al. (2011).
(5) Castle et al. (1998).
(6) see http://pacifica.pices.jp/cgi-bin/PACIFICAadjustment.csv.
(7) Tanhua et al. (2010), Pierrot et al. (2010). Also, see http://carina.geomar.de/.
[a] Calculated from DIC and $pCO_2(20)$.

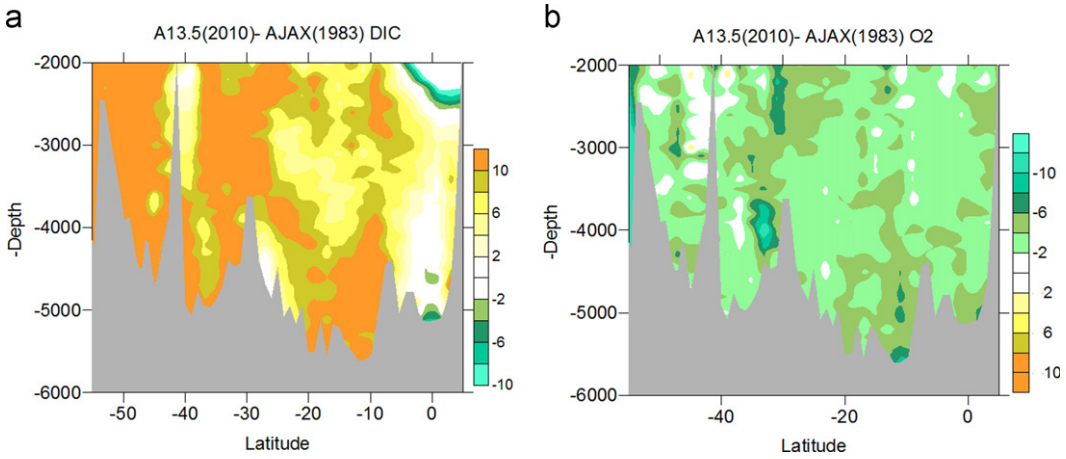

Fig. B1. Difference in DIC (a) and O_2 (b) between the AJAX cruise (1986) and the A13.5 cruise (2010) before adjustments were applied to the AJAX data (Table B1). See Fig. 3 for the corrected difference.

Fig. 3a that a simple additive correction for the cruise is not optimal.

Of note is that the P18 and A13.5 lines are the repeat hydrography lines near the boundary of the basins with a few lines crossing. As such, the procedures to determine systematic offsets in the parameters are less robust in the basin scale quality control and adjustment procedures.

References

Anderson, L.A., Sarmiento, J.L., 1994. Redfield ratios of remineralization determined by nutrient data analysis. Global Biogeochem. Cycles 8, 65–80.

Bullister, J.L., Weiss, R.L., 1988. Determination of CC13F and CC12F2 in seawater and air. Deep-Sea Res. 25, 839–853.

Brewer, P.G., Broecker, W.S., Jenkins, W.J., Rhines, P.B., Rooth, C.G., Swift, J.H., Takahashi, T., Williams, R.T., 1983. A climatic freshening of the deep Atlantic north of 50°N over the past 20 years. Science 222, 1237–1239.

Byrne, R.H., Mecking, S., Feely, R.A., Liu, X., 2010. Direct observations of basin-wide acidification of the North Pacific. Geophys. Res. Lett. 37, L02601 (http://dx.doi.org/10.1029/2009GL040999).

Castle, R., Wanninkhof, R., Doney, S.C., Bullister, J., Johns, L., Feely, R.A., Huss, B.E., Millero, F.J., Lee, K., 1998. Chemical and Hydrographic Profiles and Underway Measurements from the North Atlantic During July and August of 1993. NOAA Data Report, ERL AOML-32, p. 68.

Chen, H., Wanninkhof, R., Feely, R.A., Greeley, D., 1995. Measurement of Fugacity of Carbon Dioxide in Subsurface Water: An Evaluation of a Method Based on Infrared Analysis. NOAA Technical Report, ERL AOML-85, p. 52.

Chipman, D.W., Marra, J., Takahashi, T., 1993. Primary production at 47°N and 20°W in the North Atlantic Ocean: a comparison between the ^{14}C incubation method and mixed layer carbon budget observations. Deep-Sea Res. II 40, 151–169.

Chipman, D.W., Takahashi, T., Sutherland, S.C., 1986. Carbon Chemistry of the South Atlantic Ocean and the Weddell Sea: The Results of the Atlantic Long Lines (AJAX) expeditions, October 1983–February, 1984. National Science Foundation, Technical Report, Grant OCE-83-09987, p. 185.

DOE, 1994. Handbook of Methods for the Analysis of the Various Parameters of the Carbon Dioxide System in Seawater (version 2). In: Dickson, A.G., Goyet, C. (Eds.), ORNL/CDIAC-74. Oak Ridge National Laboratory, Carbon Dioxide Information Analysis Center, U.S. Department of Energy, Oak Ridge, Tennessee.

Doney, S.C., Large, W.G., Bryan, F.O., 1998. Surface ocean fluxes and water-mass transformation rates in the coupled NCAR climate system model. J. Clim. 11, 1420–1441.

Doney, S.C., Hecht, M.W., 2002. Antarctic Bottom Water formation and deep-water chlorofluorocarbon distributions in a global ocean climate model. J. Phys. Oceanogr. 32, 1642–1666.

Doney, S.C., Yeager, S., Danabasoglu, G., Large, W.G., McWilliams, J.C., 2007. Mechanisms governing interannual variability of upper ocean temperature in a global hindcast simulation. J. Phys. Oceanogr. 37, 1918–1938.

Doney, S.C., Lima, I., Feely, R.A., Glover, D.M., Lindsay, K., Mahowald, N., Moore, J.K., Wanninkhof, R., 2009. Mechanisms governing interannual variability in upper-ocean inorganic carbon system and air-sea CO_2 fluxes: physical climate and atmospheric dust. Deep-Sea Res. II 56, 640–655.

Friederich, G.E., Sherman, P., Codispoti, L.A., 1984. A High Precision Automated Winkler Titration System Based on a HP-85 Computer: A Simple Colorimeter and an Inexpensive Electromechanical Burette. Bigelow Lab. Technical Report 42, p. 24.

Garzoli, S.L., Boebel, O., Bryden, H., Fine, R.A., Fukasawa, M., Gladyshev, S., Johnson, G., Johnson, M., MacDonald, A., Meinen, C.S., Mercier, H., Orsi, A., Piola, A., Rintoul, S., Speich, S., Visbeck, M., Wanninkhof, R., 2010. Progressing towards global sustained deep ocean observations. In: Hall, J., Harrison, D.E., Stammer, D. (Eds.), OceanObs09: Sustained Ocean Observations and Information for Society, 2. European Space Agency Publ., pp. 12.

Gent, P.R., Danabasoglu, G., Donner, L.J., Holland, M.M., Hunke, E.C., Jayne, S.R., Lawrence, D.M., Neale, R.B., Rasch, P.J., Vertenstein, M., Worley, P.H., Yang, Z.-L., Zhang, M., 2011. The community climate system model, version 4. J. Clim. 24, 4973–4991.

Gouretski, V.V., Jancke, K., 2001. Systematic errors as the cause for an apparent deep water property variability: global analysis of the WOCE and historical hydrographic data. Prog. Oceanogr. 48 (4), 337–402.

Gruber, N., Sarmiento, J.L., Stocker, T.F., 1996. An improved method for detecting anthropogenic CO_2 in the oceans. Global Biogeochem. Cycles 10, 809–837.

Hoppema, M., Fahrbach, E., Stoll, M.H.C., de Baar, H.J.W., 1998. Increase of carbon dioxide in the bottom water of the Weddell Sea, Antarctica. Mar. Chem. 59, 201–210.

Hoppema, M., Velo, A., van Heuven, S., Tanhua, T., Key, R.M., Lin, X., Bakker, D.C.E., Pérez, F.F., Ríos, A.F., Lo Monaco, C., Sabine, C.L., Alvarez, M., Bellerby, R.G.J., 2009. Consistency of cruise data of the CARINA database in the Atlantic sector of the Southern Ocean. Earth Syst. Sci. Data 1, 63–75, http://dx.doi.org/10.5194/essd-1-63-2009.

Ilyina, T., Zeebe, R.E., Maier-Reimer, E., Heinze, C., 2009. Early detection of ocean acidification effects on marine calcification. Global Biogeochem. Cycles 23, GB1008 (http://dx.doi.org/10.1029/2008GB003278).

Ishii, M., Suzuki, T., Key, R., 2011. Pacific Ocean interior carbon data synthesis. PACIFICA. PICES Press, pp. 20–22, 〈http://www.pices.int/publications/pices_press/volume19/v19_n1/pp_20-23_PACIFICA_f.pdf〉.

Johnson, G.C., Doney, S.C., 2006. Recent western South Atlantic bottom water warming. Geophys. Res. Lett. 33 (10.1029/2006GL026769).

Johnson, K.M., Sieburth, N., Williams, B., Brandstrom, L., 1987. Coulometric total carbon dioxide analysis for marine studies: automation and calibration. Mar. Chem. 21, 117–133.

Key, R.M., Kozyr, A., Sabine, C.L., Lee, K., Wanninkhof, R., Bullister, J.L., Feely, R.A., Millero, F.J., Mordy, C., Peng, T.H., 2004. A global ocean carbon climatology: results from Global Data Analysis Project (GLODAP). Global Biogeochem. Cycles 18, GB4031. (http://dx.doi.org/10.1029/2004GB002247).

Khatiwala, S., Primeau, F., Hall, T., 2009. Reconstruction of the history of anthropogenic CO_2 concentrations in the ocean. Nature 462, 346–349 (10.1038/nature08526).

Khatiwala, S., Tanhua, T., Mikaloff Fletcher, S., Gerber, M., Doney, S.C., Graven, H.D., Gruber, N., McKinley, G.A., Murata, A., Ríos, A.F., Sabine, C.L., Sarmiento, J.L., 2012. Global ocean storage of anthropogenic carbon. Biogeosci. Discuss. 9, 8931–8988.

Körtzinger, A., Rhein, M., Mintrop, L., 1999. Anthropogenic CO_2 and CFCs in the North Atlantic Ocean: a comparison of man-made tracers. Geophys. Res. Lett. 26, 2065–2068.

Lamb, M.F., Sabine, C.L., Feely, R.A., Wanninkhof, R., Key, R.M., Johnson, G.C., Millero, F.J., Lee, K., Peng, T.-H., Kozyr, A., Bullister, J.L., Greeley, D., Byrne, R.H., Chipman, D.W., Dickson, A.G., Goyet, C., Guenther, P.R., Ishii, M., Johnson, K.M., Keeling, C.D., Ono, T., Shitashima, K., Tilbrook, B., Takahashi, T., Wallace, D.W.R., Watanabe, Y.W., Winn, C., Wong, C.S., 2002. Consistency and synthesis of Pacific Ocean CO_2 survey data. Deep-Sea Res. II 49, 21–58.

Levine, N.M., Doney, S.C., Wanninkhof, R., Lindsay, K., Fung, I.Y., 2008. The impact of ocean carbon system variability on the detection of temporal increases in anthropogenic CO_2. J. Geophys. Res., 113 (10.1029/2007JC004153).

Lewis, E., Wallace, D.W.R., 1998. Program Developed for CO_2 System Calculations. ORNL/CDIAC-105. Oak Ridge National Laboratory, Carbon Dioxide Information Analysis Center, U.S. Department of Energy, Oak Ridge, Tennessee. (21 pp).

Marion, G.M., Millero, F.J., Camoes, M.F., Spitzer, P., Feistel, R., Chen, C.T.A., 2011. pH of seawater. Mar. Chem. 126, 89–96 (10.1016/j.marchem.2011.04.002).

McElligott, S., Byrne, R.H., Lee, K., Wanninkhof, R., Millero, F.J., Feely, R.A., 1998. Discrete water column measurements of CO_2 fugacity and pH in seawater: a comparison of direct measurements and thermodynamic calculations. Mar. Chem. 60, 63–73.

Mercier, H., Speer, K.G., 1998. Transport of bottom water in the romanche fracture zone and the chain fracture zone. J. Phys. Oceanogr. 28, 779–790.

Moore, J.K., Doney, S.C., Lindsay, K., 2004. Upper ocean ecosystem dynamics and iron cycling in a global three-dimensional model. Global Biogeochem. Cycles 18, GB4028 (http://dx.doi.org/10.1029/2004GB002220).

Neill, C., Johnson, K.M., Lewis, E., Wallace, D.W.R., 1997. Small volume, batch equilibration measurement of fCO_2 in discrete water samples. Limnol. Oceanogr. 42, 1774–1783.

Peng, T.-H., Wanninkhof, R., Bullister, J., Feely, R., Takahashi, T., 1998. Quantification of decadal anthropogenic CO_2 uptake in the ocean based on dissolved inorganic carbon measurements. Nature 396, 560–563.

Pérez, F.F., Vázquez-Rodríguez, M., Louarn, E., Padín, X.A., Mercier, H., Ríos, A.F., 2008. Temporal variability of the anthropogenic CO_2 storage in the Irminger Sea. Biogeosciences 5, 1669–1679 (http://dx.doi.org/10.5194/bg-5-1669-2008).

Pérez, F.F., Vázquez-Rodríguez, M., Mercier, H., Velo, A., Lherminier, P., Ríos, A.F., 2010. Trends of anthropogenic CO_2 storage in North Atlantic water masses. Biogeosciences 7, 1789–1807.

Pierrot, D., Brown, P., van Heuven, S., Tanhua, T., Schuster, U., Wanninkhof, R., Key, R.M., 2010. CARINA TCO_2 data in the Atlantic Ocean. Earth Syst. Sci. Data 2, 177–187.

Pierrot, D., Lewis, E., Wallace, D.W.R., 2006. MS Excel Program Developed for CO_2 System Calculations. ORNL/CDIAC-105a. Oak Ridge National Laboratory, Carbon Dioxide Information Analysis Center, U.S. Department of Energy, Oak Ridge, Tennessee.

Purkey, S.G., Johnson, G.C., 2010. Warming of global abyssal and deep Southern Ocean waters between the 1990s and 2000s: contributions to global heat and sea level rise budgets. J. Clim. 23, 6336–6635 (6310.1175/2010JCLI3682.6331).

Ríos, A.F., Velo, A., Pardo, P.C., Hoppema, M., Pérez, F.F., 2011. An update of anthropogenic CO_2 storage rates in the western South Atlantic basin and the role of Antarctic Bottom Water. J. Mar. Syst. 94, 197–203 (http://dx.doi.org/10.1016/j.jmarsys.2011.11.023).

Sabine, C.L., Feely, R.A., Gruber, N., Key, R., Lee, K., Bullister, J.L., Wanninkhof, R., Wong, C.S., Wallace, D.W.R., Tilbrook, B., Millero, F.J., Peng, T.-H., Kozyr, A., Ono, T., Ríos, A.F., 2004. The oceanic sink for anthropogenic CO_2. Science 305, 367–371.

Sabine, C.L., Tanhua, T., 2010. Estimation of anthropogenic CO_2 inventories in the ocean. Annu. Rev. Mar. Sci 2, 175–198 (http://dx.doi.org/10.1146/annurev-marine-120308-080947).

Sloyan, B.M., Rintoul, S.R., 2001. The Southern Ocean limb of the global deep overturning circulation. J. Phys. Oceanogr. 31, 143–173.

Takahashi, T., Broecker, W.S., Werner, S.R., 1980. Carbonate chemistry of the surface waters of the world ocean. In: Goldberg, E.D., Horibe, Y., Saruhashi, K. (Eds.), Isotope Marine Chemistry. Uchida Rokakuho Publ. Co., Tokyo, pp. 291–326.

Tanhua, T., Biastoch, A., Körtzinger, A., Lüger, H., Boning, C., Wallace, D.W.R., 2006. Changes of anthropogenic CO_2 and CFCs in the North Atlantic between 1981 and 2004. Global Biogeochem. Cycles 20 (4), GB4017 (http://dx.doi.org/10.1029/2006GB002695).

Tanhua, T., Steinfeldt, R., Key, R.M., Brown, P., Gruber, N., Wanninkhof, R., Pérez, F., Körtzinger, A., Velo, A., Schuster, U., van Heuven, S., Bullister, J.L., Stendardo, I., Hoppema, M., Olsen, A., Kozyr, A., Pierrot, D., Schirnick, C., Wallace, D.W.R., 2010. Atlantic Ocean CARINA data overview and salinity adjustments. Earth Syst. Sci. Data 2, 17–34.

van Heuven, S., Hoppema, M., Huhn, O., Slagter, H.A., de Baar, H.J.W., 2011. Direct observation of increasing CO_2 in the Weddell Gyre along the Prime Meridian during1973–2008. Deep-Sea Res. II 58, 2613–2635.

Vázquez-Rodríguez, M., Touratier, F., Lo Monaco, C., Waugh, D.W., Padín, X.A., Bellerby, R.G.J., Goyet, C., Metzl, N., Ríos, A.F., Pérez, F.F., 2009. Anthropogenic carbon distributions in the Atlantic Ocean: data-based estimates from the Arctic to the Antarctic. Biogeosciences 6 (3), 439–451.

Wanninkhof, R., Peng, T.-H., Huss, B., Sabine, C.L., Lee, K., 2003. Comparison of Inorganic Carbon System Parameters Measured in the Atlantic Ocean from 1990 to 1998 and Recommended Adjustments. ORNL/CDIAC-140. Oak Ridge National Laboratory, Carbon Dioxide Information Analysis Center, U.S. Department of Energy, Oak Ridge, Tennessee. (45 pp).

Wanninkhof, R., Thoning, K., 1993. Measurement of fugacity of CO_2 in surface water using continuous and discrete sampling methods. Mar. Chem. 44 (2-4), 189–205.

Wanninkhof, R., Feely, R.A., 1998. fCO_2 dynamics in the Atlantic, Pacific, and South Indian oceans. Mar. Chem. 60, 15–31.

Wanninkhof, R., Doney, S.C., Bullister, J.L., Levine, N.M., Warner, M.J., Gruber, N., 2010. Detecting anthropogenic CO_2 changes in the interior Atlantic Ocean between 1989 and 2005. J. Geophys. Res. 115, C11028 http://dx.doi.org/10.1029/2010JC006251.

Weiss, R.F., 1974. Carbon dioxide in water and seawater: the solubility of a non-ideal gas. Mar. Chem. 2, 203–215.